

**CHAPTER IV: PRODUCTION OF (*R*, *S*)-RETICULINE AND
DOWNSTREAM BENZYLISOQUINOLINE ALKALOIDS IN
*SACCHAROMYCES CEREVISIAE***

Adapted from Hawkins, K.M. & Smolke, C.D. *Nat Chem Biol* **4**, 564-573 (2008)

Abstract

The benzyloquinoline alkaloids (BIAs) are a diverse class of plant secondary metabolites that exhibit a broad range of pharmacological activities and are synthesized through biosynthetic pathways that exhibit complex enzyme activities and regulatory strategies. We have engineered yeast to produce the major branch point intermediate reticuline and downstream BIA metabolites from a commercially available substrate. An enzyme tuning strategy was implemented that identified activity differences between variants and determined optimal expression levels. By synthesizing both stereoisomer forms of reticuline and integrating enzyme activities from three plant sources and humans, we demonstrated the synthesis of metabolites in the sanguinarine/berberine and morphinan branches. We also demonstrated that a human P450 enzyme exhibits a novel activity in the conversion of (*R*)-reticuline to the morphinan alkaloid salutaridine. Our engineered microbial hosts offer access to a rich group of BIA molecules and associated activities that will be further expanded through synthetic chemistry and biology approaches.

4.1. Introduction

We have engineered yeast strains expressing combinations of enzymes from three plant sources and humans as microbial hosts for the production of a wide array of BIA metabolites. In particular, we examined the ability of different combinations of three recombinant enzymes from *Thalictrum flavum* and *Papaver somniferum* to produce the early BIA metabolite reticuline from norlaudanosoline. In addition, we described a novel enzyme tuning strategy that can be generally applied to determine optimal enzyme expression levels to conserve cellular resources and improve growth and production rates without compromising pathway flux. These studies demonstrated that reticuline production levels varied from ~10 to 150 mg l⁻¹ depending on the combination of enzyme variants used, highlighting the differences in activities and interactions among pathway variants in the engineered host. We also engineered yeast strains that produce BIA metabolites along two of the major branches from reticuline: the sanguinarine/berberine branch and the morphinan branch. Expression of three downstream enzymes from *T. flavum* and *P. somniferum* and a reductase partner from *Arabidopsis thaliana* resulted in the synthesis of (*S*)-scoulerine, (*S*)-tetrahydrocolumbamine, and (*S*)-tetrahydroberberine from (*S*)-reticuline. In addition, expression of a human P450 enzyme and its native reductase partner resulted in the synthesis of salutaridine from (*R*)-reticuline, demonstrating a novel activity for this P450 enzyme. As the enzymatic activities leading to salutaridine have not yet been cloned and characterized from plant hosts⁶⁵, our synthetic pathway highlights the diversity of BIA products that can be synthesized in microbial hosts by combining activities from diverse sources.

4.2. Results

4.2.1. Synthesis of reticuline from norlaudanosoline in yeast

In native plant hosts such as *T. flavum* and *P. somniferum*, the first committed step in BIA biosynthesis is the condensation of dopamine and 4-hydroxyphenylacetaldehyde (4-HPA) catalyzed by norcoclaurine synthase (NCS) to produce (*S*)-norcoclaurine (Fig. 4.1). This natural intermediate undergoes a series of methylation reactions catalyzed by norcoclaurine 6-*O*-methyltransferase (6OMT), coclaurine-*N*-methyltransferase (CNMT), 3'-hydroxy-*N*-methylcoclaurine 4'-*O*-methyltransferase (4'OMT) and a hydroxylation reaction catalyzed by cytochrome P450 80B1 (CYP80B1) to produce the major branch point intermediate (*S*)-reticuline. (*S*)-Reticuline is converted to downstream metabolites along various branches, ultimately resulting in the synthesis of pharmacologically relevant molecules such as morphine and berberine.

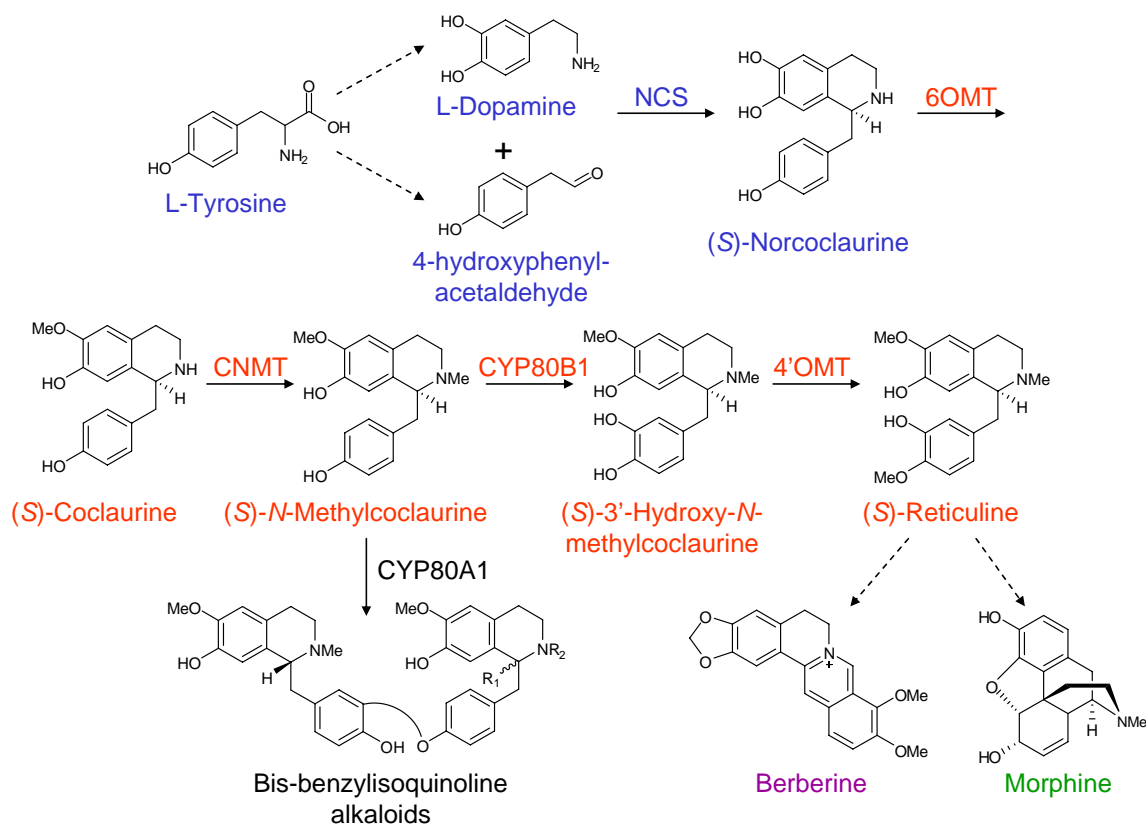


Fig. 4.1. The native BIA pathway. Color schemes for the metabolites and enzymes are as follows: upstream portion of the pathway to the first BIA backbone molecule norcoclaurine, blue; middle portion of the pathway from norcoclaurine to the branch point metabolite reticuline, red; sanguinarine/berberine branch, purple; morphine branch, green. Conversion steps for which the entire set of enzymes has not been completely elucidated or cloned are indicated by dashed arrows.

The total synthesis of the BIA backbone from tyrosine represents a significant engineering challenge as many of the plant enzymes that perform the early conversion reactions have not yet been isolated and cloned. As an alternative route, we have constructed a synthetic BIA pathway in *Saccharomyces cerevisiae* that converts the commercially available substrate (*R, S*)-norlaudanosoline to (*R, S*)-reticuline (Fig. 4.2). Norlaudanosoline differs from the natural substrate norcoclaurine by the presence of a 3'-OH group that is added to the BIA backbone by CYP80B1 in the native pathway. Therefore, our synthetic BIA pathway is comprised of three heterologous AdoMet-

dependent methyltransferase enzymes 6OMT, CNMT, and 4'OMT that convert norlaudanosoline to reticuline. Norlaudanosoline was preferred over dopamine as the starting substrate in this work as this initial conversion step proved to be extremely inefficient in yeast cells expressing either the *E. coli* or human monoamine oxidase enzyme variant with or without the *T. flavum* NCS, requiring fed dopamine concentrations of ~100 mM (data not shown).

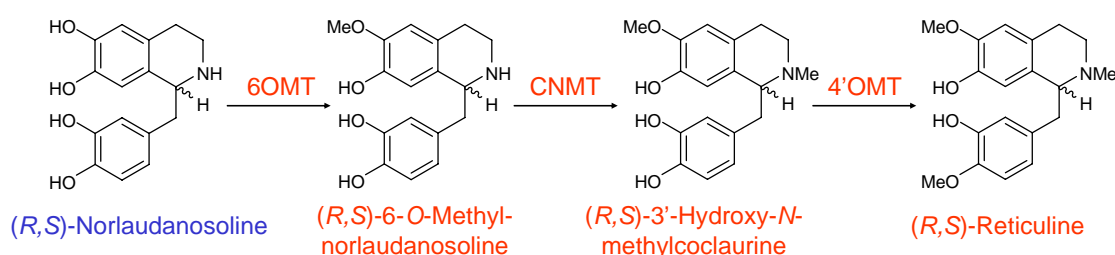


Fig. 4.2. The engineered BIA pathway for the synthesis of (*R*, *S*)-reticuline from (*R*, *S*)-norlaudanosoline. The fed substrate, (*R*, *S*)-norlaudanosoline, is indicated in blue.

Yeast strains were engineered to express one or more of the heterologous BIA pathway enzymes from *P. somniferum* and *T. flavum*. We constructed yeast BIA expression vectors, where each construct enabled the expression of one or two enzymes from constitutive TEF1 promoters (Fig. 4.3). We also constructed single-gene expression plasmids to characterize each enzyme variant individually. The resulting engineered yeast strains were grown in the presence of norlaudanosoline (or appropriate substrate) and assayed for the expected product(s).

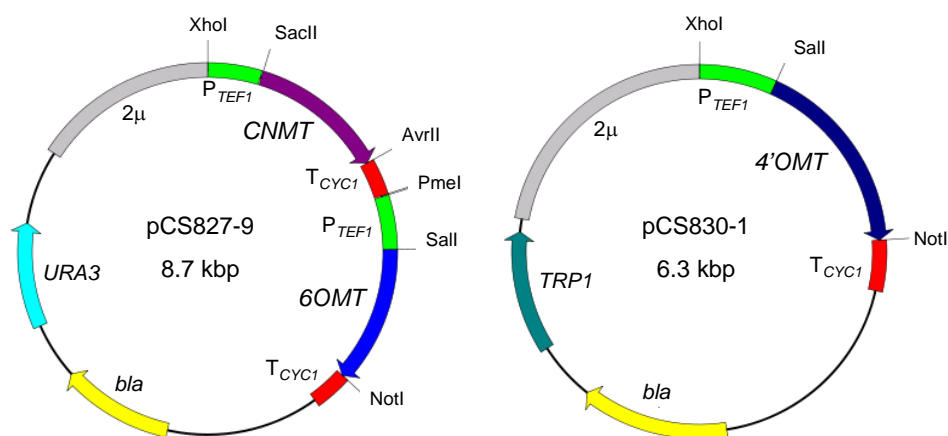


Fig. 4.3. Plasmid maps of BIA expression constructs. Heterologous cDNA sequences are expressed in yeast from constitutive TEF1 promoters on high-copy plasmids with different selection markers. The expression systems are used for the combinatorial expression of 6OMT, CNMT, and 4'OMT enzyme variants.

We tested the 6OMT and 4'OMT activities using norlaudanosoline and laudanosoline as substrates and the CNMT activities using norlaudanosoline and 6,7-dimethoxy-1,2,3,4-tetrahydroisoquinoline as substrates (Fig. 4.4). As standards are not commercially available for the metabolites of interest, following separation by high performance liquid chromatography, positive identification of BIAs was confirmed using selective reaction monitoring and tandem mass spectrometry (LC-MS/MS) in which the resulting ion fragments are characteristic for a specific molecular structure. Enzymes from both plant species performed the expected methylation reactions on the provided substrate(s) when expressed individually, and yeast strains lacking the heterologous coding sequences were not able to methylate the examined substrates. No differences were observed in the relative activities of the 6OMT and the 4'OMT variants which methylated both norlaudanosoline and laudanosoline in the expected positions. However, the *P. somniferum* CNMT variant methylated significantly more of the norlaudanosoline substrate, accumulating over six times the amount of laudanosoline compared to the *T.*

flavum variant. Conversely, the *T. flavum* variant produced ~20 times the amount of *N*-methylated 6,7-dimethoxy-1,2,3,4-tetrahydroisoquinoline, indicating the different substrate preferences of these orthologous proteins.

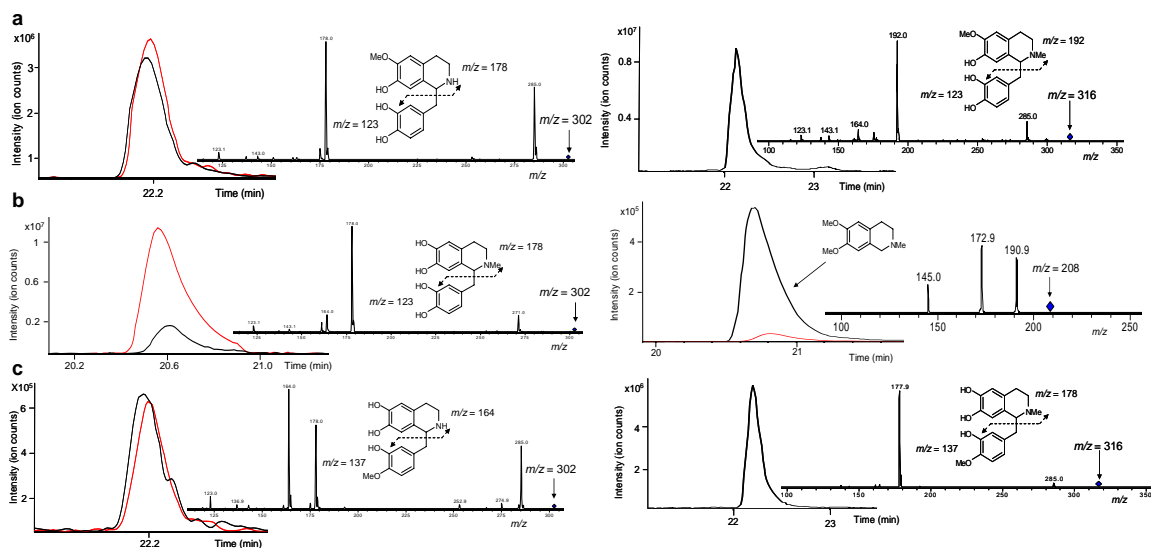


Fig. 4.4. LC-MS/MS analysis confirms individual methyltransferase activities. The growth media of engineered yeast strains supplemented with 1 mM fed substrate and grown for 48 h was analyzed for product formation. **(a)** Characterization of 6OMT fed norlaudanosoline (left) and laudanosoline (right). Left, extracted ion chromatograms for $m/z = 302$ are shown for CSY450 (red) and CSY451 (black). Right, extracted ion chromatogram for $m/z = 316$ is shown for CSY450 and is representative of CSY451. **(b)** Characterization of CNMT fed norlaudanosoline (left) and 6,7-dimethoxy-1,2,3,4-tetrahydroisoquinoline (right). Left, extracted ion chromatograms for $m/z = 302$ are shown for CSY452 (red) and CSY453 (black). Right, extracted ion chromatograms for $m/z = 208$ are shown for CSY452 (red) and CSY453 (black). **(c)** Characterization of 4'OMT fed norlaudanosoline (left) and laudanosoline (right). Left, extracted ion chromatogram for $m/z = 302$ are shown for CSY454 (red) and CSY455 (black). The 4'OMT reaction product ($m/z = 302$) appears to contain a mixture of norlaudanosoline methylated at both the 6-OH and 4'-OH positions with major fragments of $m/z = 164$ and 178 observed. The unexpected $m/z = 178$ ion is believed to be due to a co-eluting impurity in the norlaudanosoline with the parent ion $m/z = 314$. Right, extracted ion chromatogram for $m/z = 316$ is shown for CSY454 and is representative of CSY455. The fragmentation pattern of the 4'OMT reaction product does not show evidence of non-specific methylation.

We confirmed full-length expression of all methyltransferase variants by Western blotting using C-terminally tagged constructs (Fig. 4.5). Protein expression levels from

high-copy plasmids were within 2 to 3-fold of that observed from a highly-expressed yeast-enhanced GFP variant, indicating sufficient expression of the methyltransferase enzymes in the microbial host. In addition, the enzyme variants were present at similar levels such that any observed activity differences between variants cannot be attributed to differences in expression but rather some inherent property of the enzymes. The results also suggested that both CNMT variants were translated more efficiently and/or have a longer half-life in yeast compared to the 6OMT and 4'OMT enzymes.

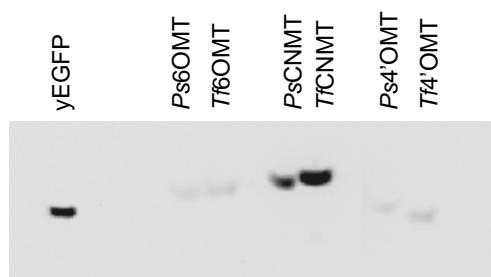


Fig. 4.5. Western blot analysis confirms protein expression of 6OMT, CNMT, and 4'OMT enzymes. Enzyme levels are comparable to levels of a yeast-enhanced GFP variant (yEGFP) expressed from the same construct (within ~2-3-fold signal). All proteins were expressed behind the TEF1 promoter on high-copy plasmids with a C-terminal V5 epitope tag. The blot was incubated with the Anti-V5 HRP antibody and a chemiluminescent assay was used for signal detection. Each lane was loaded with ~50 mg total protein. The CNMT variants are the most highly expressed and/or stable of the recombinant enzymes. At longer exposure times, degradation products were visible from the *Tf*CNMT, indicating that this protein may be subject to proteolysis in yeast, although the full-length protein still dominates.

We co-transformed yeast cells with all possible combinations of the 6OMT, CNMT, and 4'OMT enzymes from *T. flavum* and *P. somniferum* (Table 4.1). All strains harboring different combinations of the three methyltransferase enzyme variants demonstrated production of reticuline from norlaudanosoline as verified through LC-MS/MS (Fig. 4.6a). Certain enzyme combinations exhibited greater reticuline accumulation as estimated by percent conversion or the ratio of the extracted ion

chromatogram peak areas of reticuline to norlaudanosoline (Fig. 4.6b). Notably all but one strain containing the *T. flavum* CNMT variant produced ~60% less reticuline than the strains with the *P. somniferum* CNMT variant, indicating that the latter variant demonstrated higher activity in this synthetic pathway. This activity difference can be attributed to differences in substrate affinities of the CNMT variants observed in the single enzyme studies as the *P. somniferum* CNMT exhibited higher activity on the pathway substrate norlaudanosoline (Fig. 4.4). Measurements of 5-10% conversion of norlaudanosoline agreed with other estimates of reticuline concentration of ~100 μ M (from 1 mM norlaudanosoline) based on comparative peak area analysis of structurally similar standards. Although BIA metabolites up to reticuline exist only in the (*S*)-conformation in plants, our studies demonstrated that the three methyltransferases accepted both stereoisomers as substrates equally *in vivo* to yield a racemic mixture of (*R*, *S*)-reticuline from (*R*, *S*)-norlaudanosoline^{66,67} (Fig. 4.6c).

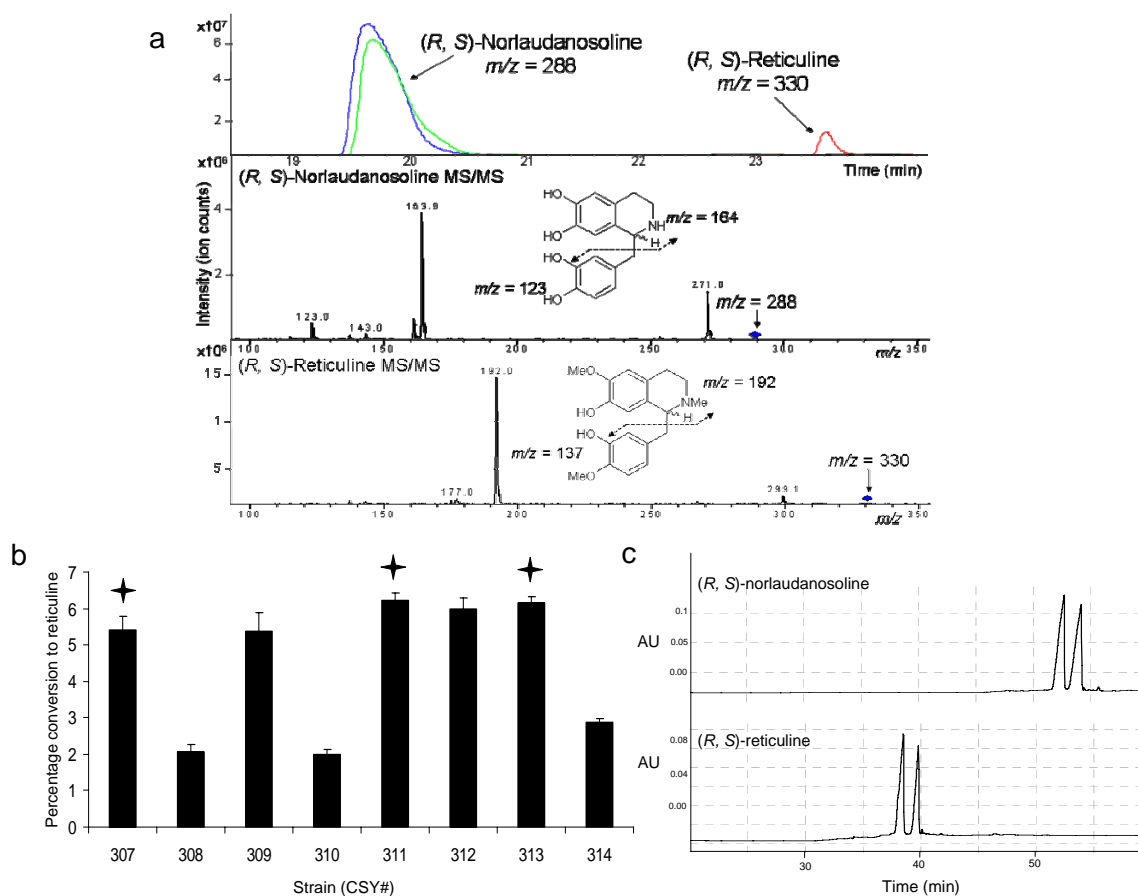


Fig. 4.6. Microbial production of (*R, S*)-reticuline. **(a)** LC-MS/MS analysis of the growth media of engineered yeast strains supplemented with 1 mM norlaudanosoline and grown for 48 h confirms reticuline production. Extracted ion chromatograms are shown for norlaudanosoline in the wild-type (blue) and CSY307 (green) strains and for reticuline in the wild-type (black, no visible peak) and CSY307 (red) strains. Reticuline is identified as the $m/z = 330$ ion eluting at 23.6 min showing the expected fragments $m/z = 192$ and 137 produced by cultures of CSY307 and similar engineered strains. Control experiments in which strains were missing any one of the three required enzymes or grown in the absence of substrate did not accumulate the metabolite peak identified as reticuline. **(b)** Reticuline production is dependent on the combination of enzyme variants expressed by the engineered yeast strains. Reticuline production is reported as percentage substrate conversion from engineered yeast strains harboring BIA expression constructs for combinatorial expression of different 6OMT, CNMT, and 4'OMT enzyme variants supplemented with 1 mM norlaudanosoline and grown for 48 h. Stars indicate enzyme combinations used in strains for stable expression. Data are reported as mean values \pm s.d. from at least three independent experiments. **(c)** Chiral analysis of (*R, S*)-norlaudanosoline and (*R, S*)-reticuline (converted by CSY288). Separation of stereoisomers was performed through capillary electrophoresis on reticuline fractions collected from the LC column.

Estimation of BIA metabolite levels in the growth media and cell extract indicated that the norlaudanosoline concentration drop across the membrane was ~10- to 30-fold and that the reticuline to norlaudanosoline ratio was slightly greater inside the cell compared to the growth media (Fig. 4.7). The results supported a passive diffusion transport mechanism in the microbial host and confirmed that the substrate was accessible to the intracellular BIA enzymes and that the synthesized metabolites accumulated in the growth media. This property greatly simplifies metabolite profiling as production levels can be estimated by direct analysis of the growth media without rigorous extraction or purification steps. However, the transport of BIA substrates across the cell membrane is somewhat limiting and highlights the importance of reconstructing this pathway in a single microbial host to avoid inefficiencies due to transport of metabolites across two cell membranes.

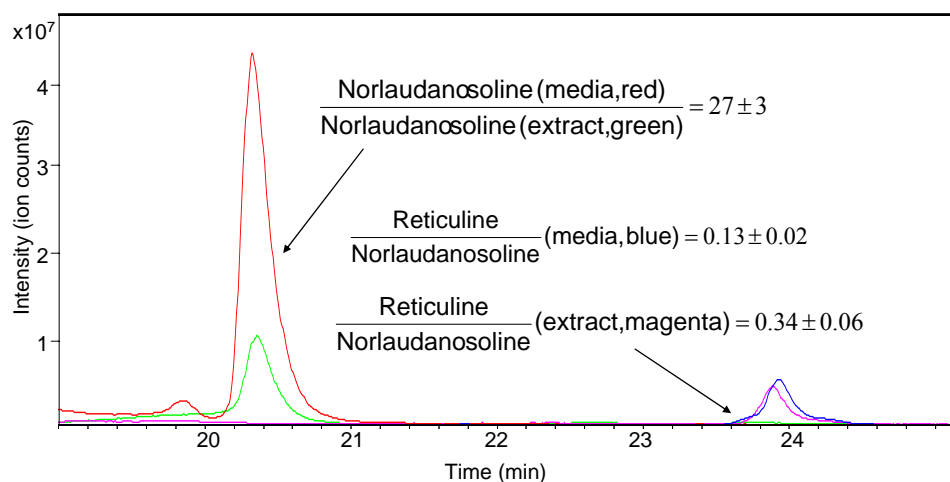


Fig. 4.7. BIA metabolites accumulate in the growth media. Analysis of norlaudanosoline (substrate) and reticuline (product) concentrations in cell extracts and growth media support a passive diffusion transport mechanism for BIA metabolites. Data shown is a 1:10 dilution of the growth media (norlaudanosoline, red; reticuline, blue) and a ~1:2 dilution of the cell extract (norlaudanosoline, green; reticuline, magenta) of CSY288 supplemented with 1 mM norlaudanosoline and grown for 48 h. Ratios of product to substrate and extracellular versus intracellular norlaudanosoline concentrations are shown

as calculated by LC-MS peak areas. Chromatograms and calculations are representative of two independent experiments \pm s.d.

In an attempt to overcome transport limitations, we deleted several identified multi-drug transporters which may be actively transporting the substrate out of the cell. Using a reticuline producing background strain CSY288, total gene deletions were made for *aqr1* Δ , *flr1* Δ , *qdr1/2* Δ , *qdr3* Δ and the quintuple knockout. The *PDR1* transcription factor known to activate expression of additional proteins from this multi-drug transport family was also deleted in the CSY288 background strain. No difference in norlaudanoline conversion was observed in any of these strain backgrounds (data not shown). However, deletion of these genes may also cause more reticuline to be retained inside the cells such that no net effect is observed in the growth media. Another approach is to express a protein which actively, and preferably selectively, transports BIA substrates into the cell but a good target candidate has not yet been identified.

4.2.2. BIA production in the yeast strains is substrate limited

We selected three combinations of the methyltransferase enzyme variants that demonstrated high conversion of norlaudanoline to reticuline for stable expression in yeast (CSY288, CSY334, CSY456; Table 4.1). Expression of heterologous enzymes from the chromosome is anticipated to result in more consistent and stable expression over time, facilitate expansion of the synthetic pathway, and enable cultures to be grown in rich media without selective pressure. However, expression levels from chromosomal integrations are expected to be lower than those from the high-copy plasmid system due to the reduction in DNA copy number. Reticuline production levels compared favorably

in all stable expression strains with only one combination of enzymes showing a decrease in production greater than 30% upon integration of the constructs (Fig. 4.8a). The results indicated that the *P. somniferum* 6OMT variant outperformed the *T. flavum* variant at lower expression levels and exhibited higher specific activity in the synthetic pathway.

The results from the analysis of reticuline production in the stable expression strains suggested that substrate conversion was not severely hindered by enzyme expression levels. We examined the effects of substrate concentration and growth phase on reticuline production levels from cultures of CSY288. Reticuline accumulation increased roughly in proportion to the initial concentration of norlaudanosoline in the media between 0.5 to 5 mM such that percent conversion was between 7-10% in all samples, supporting a substrate limitation model (Fig. 4.8b). Substrate limitation in our synthetic BIA pathway was not unexpected since, in addition to potential transport issues, norlaudanosoline and 6-*O*-methyl norlaudanosoline are not the natural substrates for 6OMT and CNMT, respectively. For example, kinetic characterization studies on the 6OMT variant from *C. japonica* determined a K_m value of 2.23 mM for (*R, S*)-norlaudanosoline, with a relative activity of 76% compared to (*S*)-norcoclaurine⁶⁶. Although the 6OMT variant from *P. somniferum* used here has a reported K_m value of 10 μ M for norcoclaurine⁶⁷, the value may be significantly higher for norlaudanosoline. We also examined the time scale of production under conditions that model a batch fermentation run and observed significant reticuline production shortly after substrate addition to a shake flask culture seeded with CSY288. The production rate slowed over time, but reticuline continued to accumulate as cells entered the stationary growth phase (Fig. 4.8c).

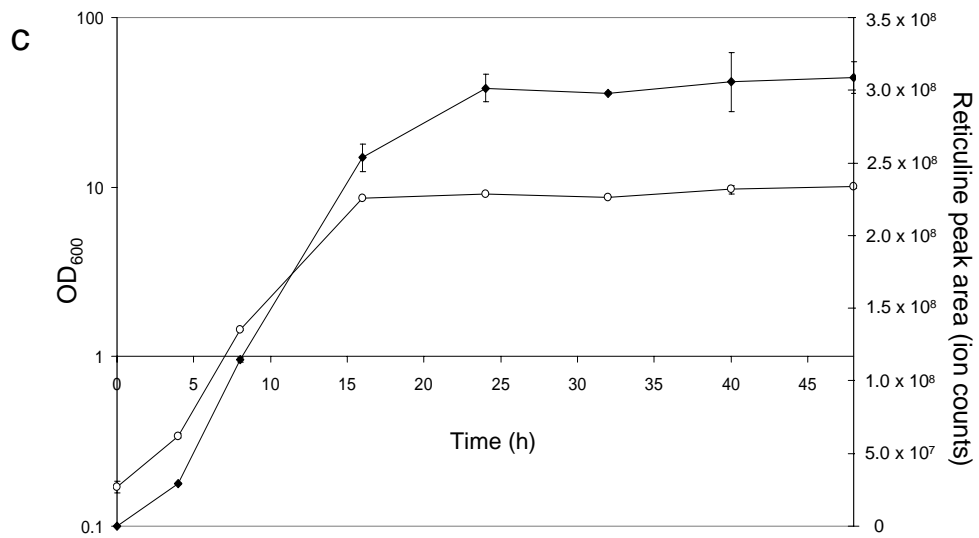
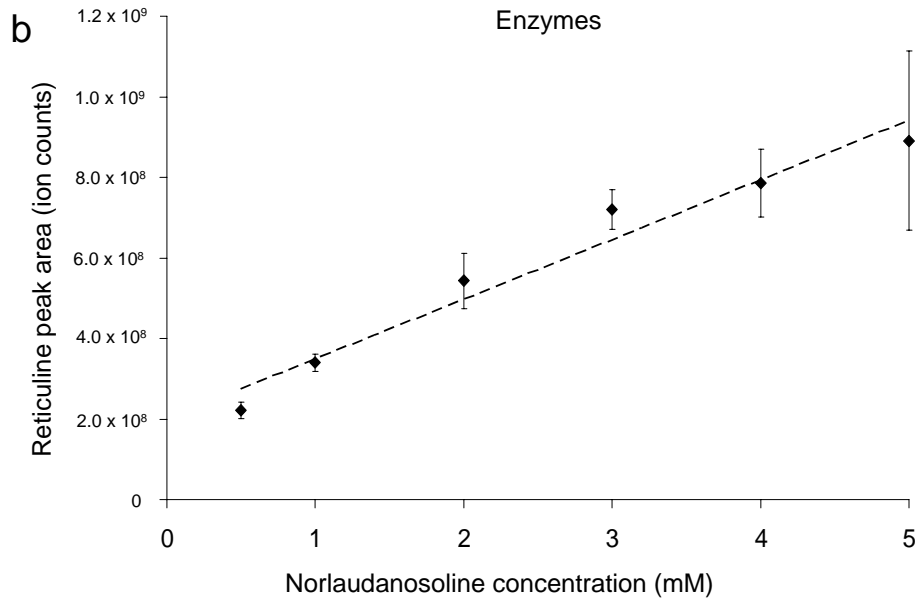
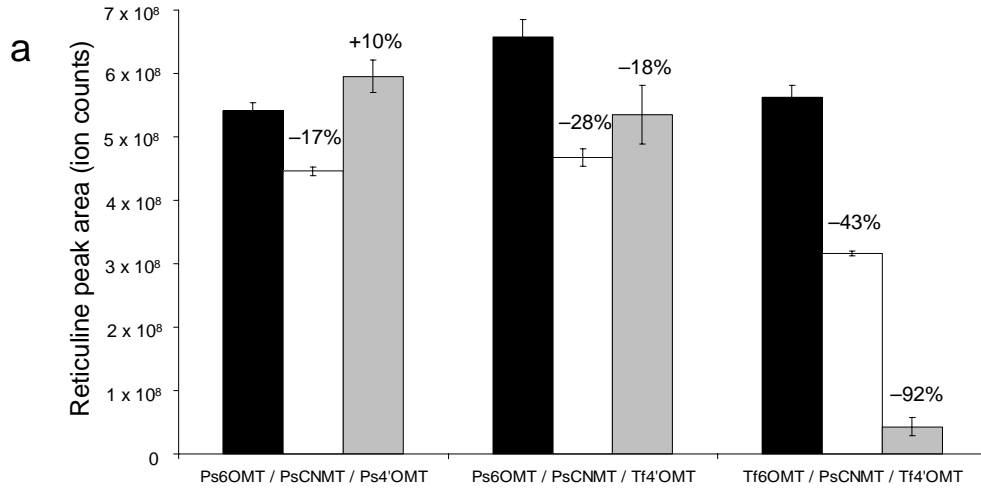


Fig. 4.8. Effects of enzyme levels, substrate levels, and culture time on reticuline production. **(a)** Reticuline production is not significantly impacted at lower enzyme expression levels. Reticuline production as measured by LC-MS peak area from three strains engineered to stably express the indicated enzyme variants from the TEF1 promoter (CSY288, CSY334, CSY456; white) or the mutant TEF7 promoter (CSY448, CSY449, and CSY458; gray) were compared to strains expressing the enzymes from plasmid-based constructs (CSY307, CSY311, CSY313; black). The percentage change in production observed from the stable strains after 48 h growth in media supplemented with 2 mM norlaudanosoline is indicated. **(b)** Reticuline production increases with substrate concentration. Reticuline production was measured in the growth media of CSY288 supplemented with a range of norlaudanosoline concentrations after 48 h growth. **(c)** Reticuline production increases with the OD₆₀₀ of the culture. Reticuline production (solid diamonds) and OD₆₀₀ (open circles) were measured at the indicated time points in the growth media of CSY288 supplemented with 2 mM norlaudanosoline added at $t = 0$. All data are reported as mean values \pm s.d. from at least three independent experiments.

4.2.3. Tuning enzyme levels with a novel titration strategy

Pathway optimization strategies often require an analysis of enzyme expression levels and their effects on metabolite accumulation and strain growth rate. Systems that enable heterologous enzymes to be expressed at a minimum level while maintaining maximum pathway flux and product accumulation are desired to avoid wasting cellular resources synthesizing excess proteins. Such strategies become more critical as an engineered pathway is extended to include additional enzymes that will further tax cellular resources. Optimization of pathway enzyme levels should result in an improved strain growth rate and a markedly reduced production time.

To optimize BIA enzyme expression levels, we developed a system that allows each enzyme to be titrated independently. We replaced the constitutive TEF1 promoter with the GAL1-10 galactose-inducible promoter for one of the three BIA enzyme coding sequences in our stable strains to allow tunable expression of one heterologous enzyme while holding the other two constant. In addition, we deleted the GAL2 permease from

each strain to enable titratable control over enzyme levels. Deletion of the *GAL2* permease has been previously shown to result in a more homogenous, linear induction response from the GAL network relative to the wild type all-or-none, switch-like response³. Our system design resulted in a series of engineered strains stably expressing the BIA enzymes in which levels of one of the three methyltransferases were precisely regulated according to galactose concentration (CSY325-329; Table 4.1).

We used the tunable strains to determine relationships between galactose concentration, enzyme expression levels, and reticuline production. The titratable yeast strains were grown in 1 mM norlaudanosoline and varying galactose concentrations, and reticuline production was analyzed at 24 h after substrate addition. The enzyme titration experiments demonstrated that in nearly all strains at ~0.5% galactose, conversion of norlaudanosoline to reticuline reached over 70% of the levels attained from fully induced conditions at 2% galactose (Fig. 4.9a). All strains demonstrated production comparable to the parent strains at maximum induction levels. Only the strain containing the GAL-inducible *T. flavum* 6OMT (CSY329; Table 4.1) did not show changes in production corresponding to galactose concentration as reticuline production was similarly low at all points, suggesting that higher expression levels were necessary to observe significant activity of this variant in our system (data not shown).

The relationship between galactose concentration and relative expression levels was obtained indirectly using an analogous fluorescent reporter system. We constructed integration cassettes containing a green fluorescent protein (yEGFP3) under the control of the constitutive *TEF1* promoter or the inducible *GAL1-10* promoter in a *GAL2Δ* background to make strains CSY428 and CSY429 (Table 4.1). We compared the relative

fluorescence levels from the GAL1-10 promoter at various galactose concentrations to fluorescence levels observed from the TEF1 promoter. The reporter protein titration experiments demonstrated that the expression from the tunable GAL promoter system at 0.5% galactose translated to ~16% expression relative to the native TEF1 promoter (Fig. 4.9b). The results indicated that the transcriptional activity of the heterologous enzyme promoters could be significantly reduced while maintaining maximal substrate conversion to reticuline.

We optimized BIA enzyme expression levels based on our titration assay results by designing integration cassettes in which the level of expression from the promoter system was minimized without compromising production. We used a mutated TEF promoter library⁵ in which TEF1 promoter variants with altered levels of gene expression had been generated and characterized. Our titration assays indicated that optimal expression levels for each of the BIA enzymes tested, with the possible exception of *P. somniferum* 4'OMT, corresponded to ~16% of the native TEF1 promoter, approximating that of the TEF7 mutant. We replaced the TEF1 promoter with the TEF7 promoter in our chromosomal integration cassettes and constructed optimized reticuline-producing strains. TEF7-substituted versions of CSY288 and CSY334 (CSY448, CSY449; Table 4.1) showed comparable production levels (Fig. 4.8a). However, CSY458 showed greatly reduced production compared to CSY456 and other TEF7-substituted strains. Since the only difference between CSY458 and CSY449 is the 6OMT variant, the data further supported that this step can become limiting at low expression levels and that the *P. somniferum* 6OMT exhibited higher specific activity than the *T. flavum* variant in the synthetic pathway. We verified trends in relative transcript levels between the TEF1 and

TEF7 integrated expression systems and the high copy plasmid-based system by qRT-PCR (Fig. 4.9c). Growth rates were not significantly and reproducibly different between the TEF1 and TEF7 strains; however, this optimization strategy, which resulted in reduced metabolic load on the cell without compromising reticuline production levels, will likely prove more important upon further extensions of the pathway. In addition, this tuning strategy can be generally applied to other recombinant pathways in yeast to determine and set the minimal expression level of heterologous enzymes for a desired product yield.

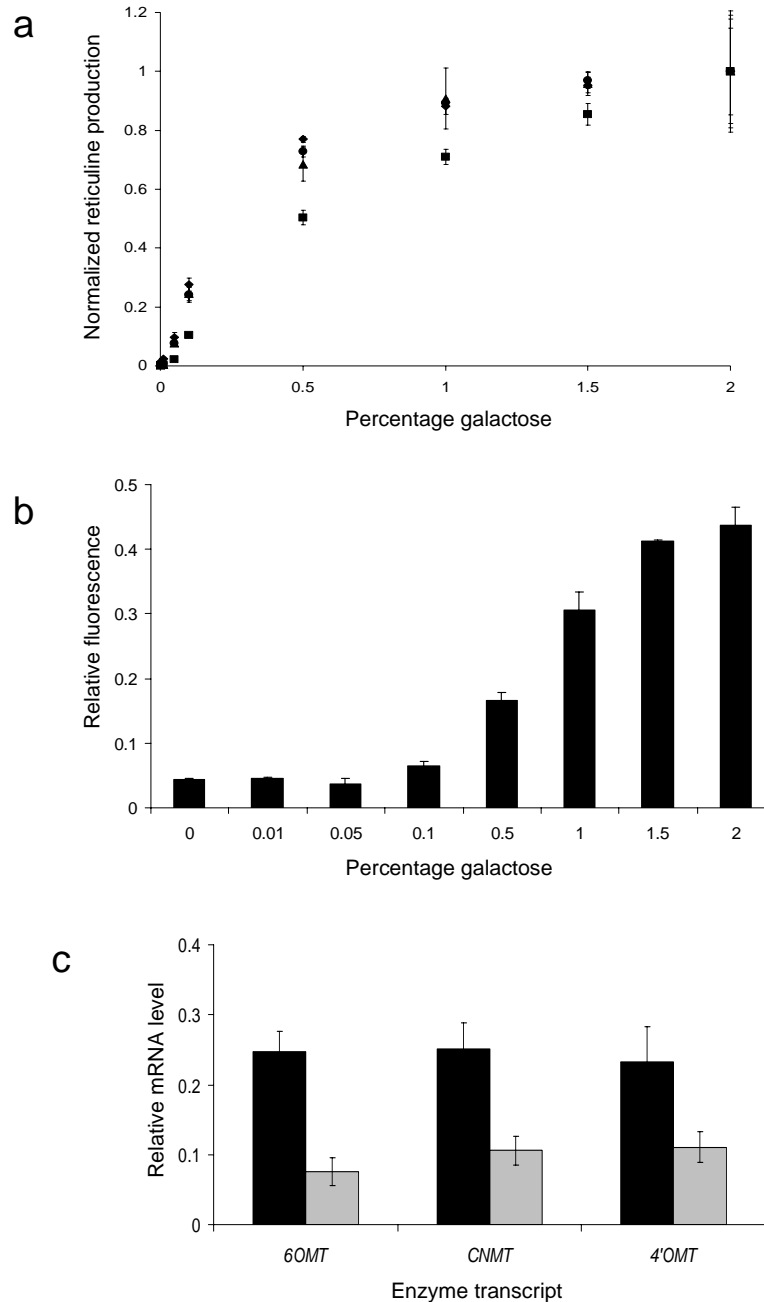


Fig. 4.9. A novel strategy for tuning enzyme expression levels. **(a)** Reticuline production as a function of galactose concentration in engineered reticuline-producing strains expressing one heterologous enzyme from the titratable GAL expression system; production is normalized to each strain in 2% galactose. CSY325, diamonds; CSY326, squares; CSY327, circles; CSY328, triangles. Cells were grown overnight in noninducing-nonrepressing media and backdiluted into media containing the indicated galactose concentration. Following 4 h of induction, 1 mM norlaundanosoline was added and supernatants were analyzed for reticuline production after 24 h. **(b)** GFP reporter strains were used to guide the determination of relative protein expression levels for the enzyme titration studies. Relative fluorescence data is reported for CSY429 normalized to

CSY428. Cells were grown overnight in noninducing-nonrepressing media and backdiluted into media containing the indicated galactose concentration. Fluorescence measurements were normalized to OD₆₀₀ for each sample and taken during the exponential growth phase. (c) qRT-PCR analysis confirms trends in relative transcript levels from the TEF1 and TEF7 integrated expression systems compared to the high-copy plasmid-based systems. Transcript levels in representative stable strains using the TEF1 promoter (CSY288; black) and the TEF7 promoter (CSY448; gray) are normalized to levels from a high-copy plasmid expression system (CSY307). All data are reported as mean values \pm s.d. from at least two independent experiments.

4.2.4. Synthesis of sanguinarine/berberine intermediates

Reticuline represents a major branch point intermediate in plant secondary metabolism from which a wide variety of BIA metabolites can be derived, including sanguinarine, berberine, protopine, magnoflorine, and morphinan alkaloids. The enzymes in these downstream BIA branches are of particular interest as many exhibit complex biosynthetic activities. We examined the synthesis of metabolites along a major branch, the sanguinarine/berberine branch, by expressing additional enzymes from the native plant pathways as a demonstration of the diverse natural products and activities that can be produced in our engineered yeast strains. This family of benzophenanthridine alkaloids has generated interest for their pharmacological activities, most notably as antimicrobial agents.

The first conversion step in the sanguinarine/berberine branch of the BIA pathway is performed by the berberine bridge enzyme (BBE), which catalyzes the oxidative cyclization of the N-methyl moiety of (*S*)-reticuline into the berberine bridge carbon of (*S*)-scoulerine⁶⁸ (Fig. 4.10a). This unique reaction forms the protoberberine carbon skeleton via a methylene iminium ion intermediate and cannot be replicated through synthetic chemistry approaches. We constructed a plasmid expressing the *P. somniferum* BBE cDNA for transformation into our reticuline-producing yeast strains CSY288 and

CSY334 (CSY336, CSY338; Table 4.1). LC-MS/MS analysis demonstrated that the engineered strains produce (*S*)-scoulerine (Fig. 4.10b). The relative peak areas of the appropriate ions indicated ~40% conversion of (*R, S*)-reticuline to (*S*)-scoulerine with an effective conversion of ~80% based on an equal mixture of stereoisomers. In addition, we also tested enzyme truncations of the first 25 and 41 amino acids to remove the N-terminal signal sequence⁶⁹. Neither truncated variant demonstrated increased production of (*S*)-scoulerine, and the Δ 41 truncation showed slightly compromised production (Fig. 4.11).

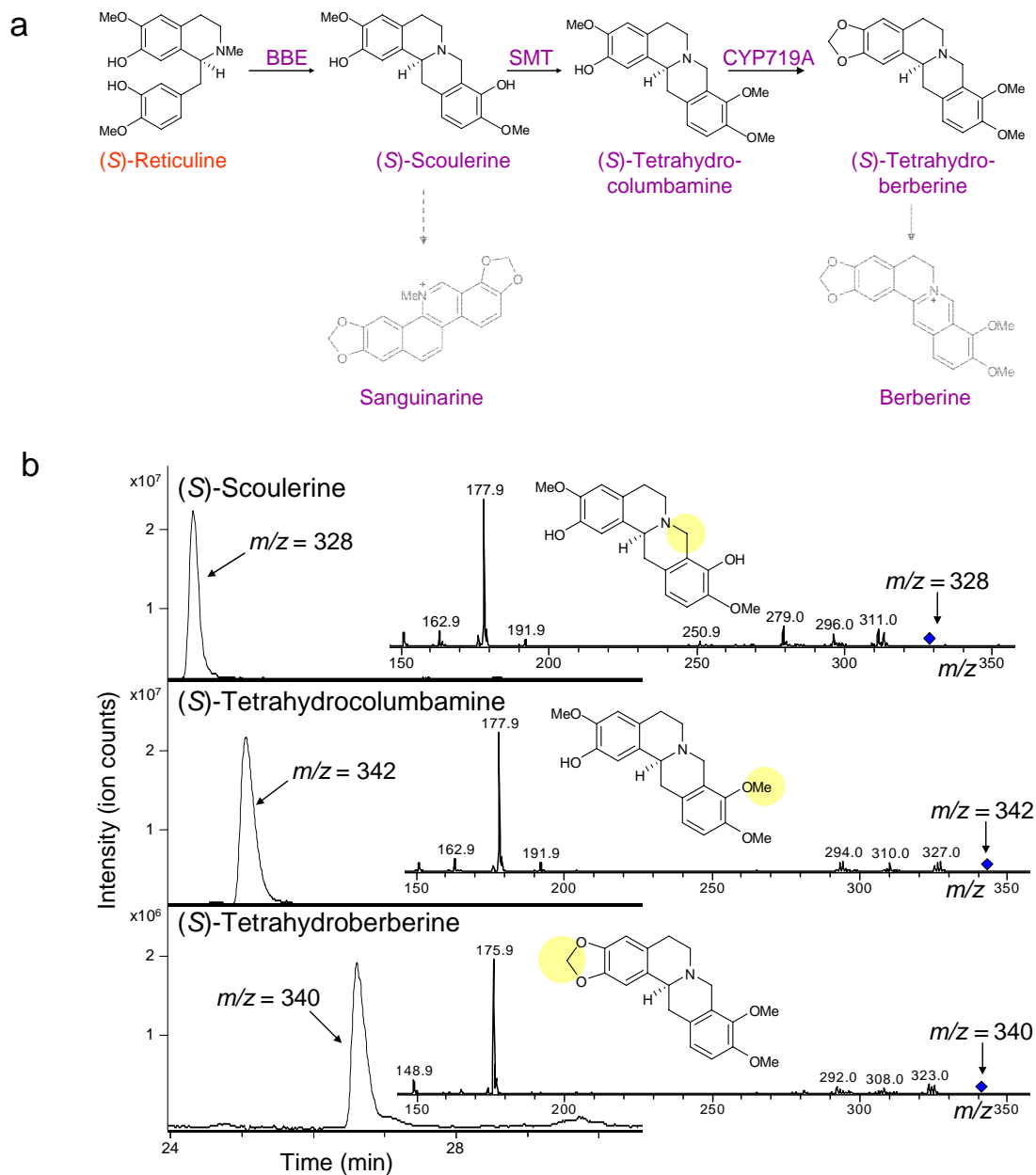


Fig. 4.10. Microbial production of BIA metabolites along the sanguinarine and berberine branches. **(a)** Pathway for the synthesis of sanguinarine/berberine metabolites from the key intermediate (*S*)-reticuline. Color schemes follow that defined in Fig. 4.1. Shaded portions of the pathway indicate steps not reconstructed in the engineered microbial host. Dashed arrows represent multiple steps and solid arrows where no enzyme is listed indicated a single step for which the enzyme has not been cloned from plant hosts. **(b)** LC-MS/MS analysis of the growth media of engineered yeast strains supplemented with 4 mM norlaudanosoline and grown for 48 h confirms (*S*)-scoulerine, (*S*)-tetrahydrocolumbamine, and (*S*)-tetrahydroberberine production. Data is shown for CSY336, CSY337, and CSY410, respectively, and is representative of analogous strains. The fragmentation pattern of the 328 ion corresponding to (*S*)-scoulerine differs

significantly from that of (*S*)-reticuline as the formation of the berberine bridge stabilizes (*S*)-scoulerine so that it does not fragment into the benzyl and isoquinoline moieties, but instead loses methyl and hydroxyl groups. The fragmentation pattern of the 342 ion identified as (*S*)-tetrahydrocolumbamine is consistent with that of the parent molecule (*S*)-scoulerine; the observed fragments exhibit an increase ($m/z = 14$) attributable to the additional methyl group. (*S*)-Tetrahydroberberine is identified by its major ion ($m/z = 340$) and exhibits a fragmentation pattern similar to the parent molecule (*S*)-tetrahydrocolumbamine; the observed fragments show a decrease ($m/z = 2$) consistent with the formation of the methylenedioxy bridge. Growth media of strains lacking the required enzyme coding sequence(s) did not display the identified metabolite peak(s).

(*S*)-Scoulerine represents a second important branch point metabolite as it can be converted to BIA metabolites along either the sanguinarine or berberine branches (Fig. 4.10a). The oxidation of (*S*)-scoulerine to (*S*)-cheilanthifoline, an intermediate metabolite along the sanguinarine branch, is catalyzed by a cytochrome P450 enzyme that has not yet been cloned from native plant hosts. Alternatively, the methylation of (*S*)-scoulerine in the 9-OH position by (*S*)-scoulerine 9-*O*-methyltransferase (SMT) results in the synthesis of (*S*)-tetrahydrocolumbamine, an intermediate metabolite along the berberine branch. We constructed a plasmid co-expressing the *P. somniferum* *BBE* and *T. flavum* *SMT* cDNAs for transformation into our reticuline-producing yeast strains (CSY337, CSY339; Table 4.1). LC-MS/MS analysis demonstrated that the heterologous SMT enzyme performed the expected methylation reaction to produce (*S*)-tetrahydrocolumbamine (Fig. 4.10b). Yeast strains producing (*S*)-tetrahydrocolumbamine from (*R, S*)-norlaudanosoline exhibited little or no accumulation of (*S*)-scoulerine, indicating efficient conversion of the substrate and yielding $\sim 60 \text{ mg l}^{-1}$ (*S*)-tetrahydrocolumbamine from 4 mM (*R, S*)-norlaudanosoline.

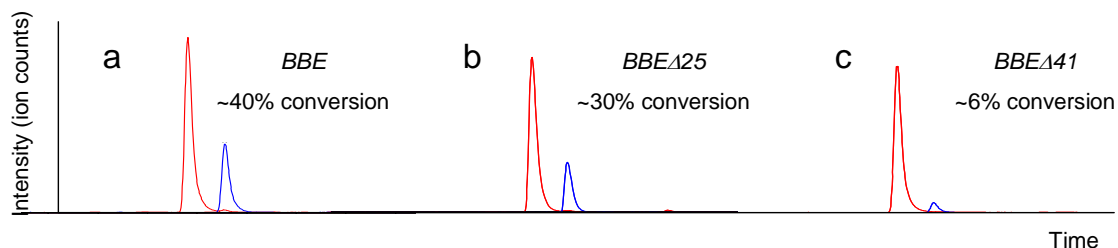


Fig. 4.11. Comparison of BBE N-terminal truncations. Extracted ion chromatograms are shown for reticuline ($m/z = 330$, red) and scoulerine ($m/z = 328$, blue). Percentage conversion is calculated as the ratio of scoulerine to reticuline measured in the growth media and values for each BBE variant are shown.

The next and penultimate metabolite along the berberine branch is (*S*)-tetrahydroberberine, or (*S*)-canadine, which is produced by a methylenedioxy bridge-forming reaction from (*S*)-tetrahydrocolumbamine (Fig. 4.10a). This reaction is catalyzed by canadine synthase, a cytochrome P450 enzyme (CYP719A1), which has been cloned from multiple berberine-producing plants⁷⁰. Previous characterization studies on the *C. japonica* CYP719A1 have been performed in a yeast strain that co-expresses the *Arabidopsis thaliana* P450 reductase ATR1⁷⁰. We therefore constructed a dual-expression plasmid containing the *T. flavum* CYP719A1 and *SMT* cDNAs for co-transformation with plasmids containing the *A. thaliana* ATR1 and *P. somniferum* BBE cDNAs into our reticuline-producing yeast strains (CSY399, CSY400; Table 4.1). LC-MS/MS analysis demonstrated low levels of (*S*)-tetrahydroberberine production ($\ll 5$ mg l⁻¹) from a starting substrate concentration of 4 mM norlaudanosoline. Production of (*S*)-tetrahydroberberine was confirmed not only by its characteristic fragmentation pattern but also by co-elution experiments with authentic (*R, S*)-tetrahydroberberine (Fig. 4.12).

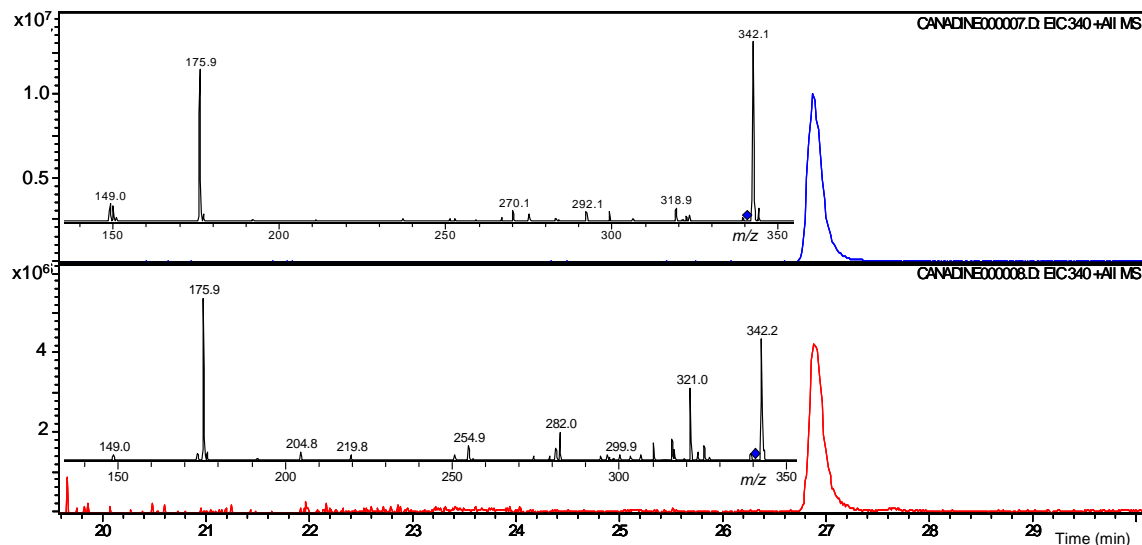


Fig. 4.12. Comparison of synthesized (*S*)-tetrahydroberberine to standard. Authentic DL-canadin or (*R*, *S*)-tetrahydroberberine (Apin Chemicals Ltd) co-elutes with the product identified as (*S*)-tetrahydroberberine synthesized by engineered yeast cells at 26.9 min using the method described. The $m/z = 340$ extracted ion chromatograms are shown for the standard (50 mM; blue) and for the yeast growth media of CSY410 supplemented with 4 mM norlaudanoline (red). MS/MS on the 340 ions shows the major ions $m/z = 149$ and $m/z = 175$ in common.

Similar analysis of engineered strains expressing endogenous levels of the yeast P450-NADPH reductase or additional copies of the yeast or human reductase did not demonstrate (*S*)-tetrahydroberberine production, suggesting that these CPR1 variants were not suitable reductase partners for CYP719A1 (data not shown). We also constructed a strain in which the *A. thaliana* *ATR1* reductase coding sequence was integrated into the chromosome of CSY288 and transformed with the plasmids expressing BBE, SMT, and CYP719A (CSY410; Table 4.1). LC-MS/MS analysis demonstrated that (*S*)-tetrahydroberberine accumulation was ~10-fold greater in CSY410 than strains with plasmid-based *ATR1* expression (Fig. 4.10b). We estimated (*S*)-tetrahydroberberine production to be ~30 mg l⁻¹ from a substrate concentration of 4 mM or ~1-2% total conversion from norlaudanoline or laudanoline prior to optimization

of this heterologous seven-enzyme pathway. The accumulation of several intermediates in the synthetic pathway highlighted remaining flux limitations in our system (Fig. 4.13).

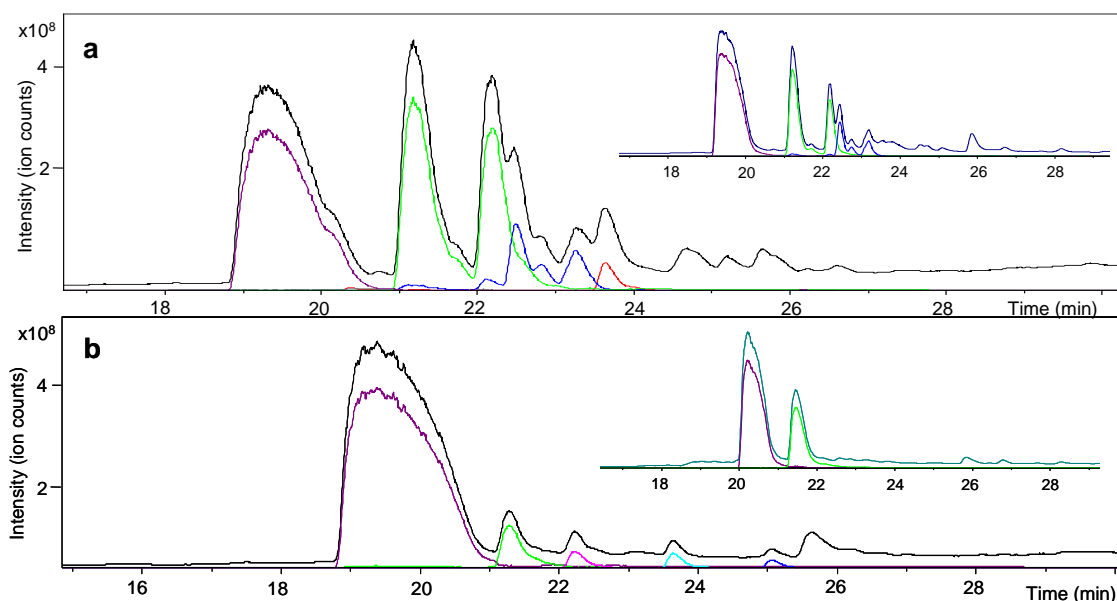


Fig. 4.13. Chromatograms show impurities and incomplete conversion of intermediates. LC-MS chromatograms of the growth media of (a) CSY288 supplemented with 2 mM norlaudanosoline and (b) CSY410 supplemented with 2 mM laudanosoline and grown for 48 h showing impurities and degradation products in the sample. (a) The total ion chromatogram is shown in black and the extracted ion chromatogram for norlaudanosoline (MS 288) is shown in purple. The major impurities are MS 314 shown in green and MS 316 shown in blue; reticuline (MS 330) is shown in red. The same 314 and 316 ions are observed in the wild-type strain supplemented with norlaudanosoline (inset). (b) The total ion chromatogram is shown in black and the extracted ion chromatogram for laudanosoline (MS 302) is shown in purple. The major impurity is MS 300 shown in green; the intermediate methyl-laudanosoline (MS 316) is shown in magenta; the intermediate reticuline (MS 330) is shown in cyan; and the intermediate tetrahydrocolumbamine (MS 342) is shown in blue. The same 300 ion is observed in the wild-type strain supplemented with laudanosoline (inset). All detectable BIA metabolites elute in this time frame with the rest of the spectra relatively flat.

4.2.5. *N*-methylation of (*S*)-tetrahydroberberine for the production of a noscapine pathway intermediate

Another rare biochemical reaction was demonstrated in our engineered yeast strains to produce a quaternary ammonium alkaloid. The tetrahydroprotoberberine *cis*-*N*-methyltransferase (TNMT) was recently cloned from opium poppy⁷¹. The native

substrate was identified as (*S*)-stylopine as this enzyme was implicated in protopine and sanguinarine biosynthesis. TNMT catalyzes the AdoMet-dependent methylation of the tertiary nitrogen of (*S*)-stylopine or similar substrate to produce a quaternary ammonium alkaloid. While exhibiting significant sequence similarity to CNMT, TNMT is the only *N*-methyltransferase in alkaloid metabolism known to produce a quaternary amine. Characterization studies of recombinant TNMT purified from *E. coli* showed a strict substrate requirement for dimethoxy or methylenedioxy functional groups at C2/3 and C9/10. The product (*S*)-tetrahydroberberine meets this requirement and TNMT was actually shown to have slightly greater activity on this substrate as opposed to stylopine⁷¹.

TNMT activity was tested in our engineered yeast strains expressing 6OMT, CNMT, and 4'OMT to produce reticuline and BBE, SMT, CYP719A/ATR1 to produce (*S*)-tetrahydroberberine. Although levels of the substrate (*S*)-tetrahydroberberine are relatively low in this extensive pathway, the correct reaction product was still detectable in the growth media. The extracted ion chromatograms and fragmentation results are shown (Fig. 4.14).

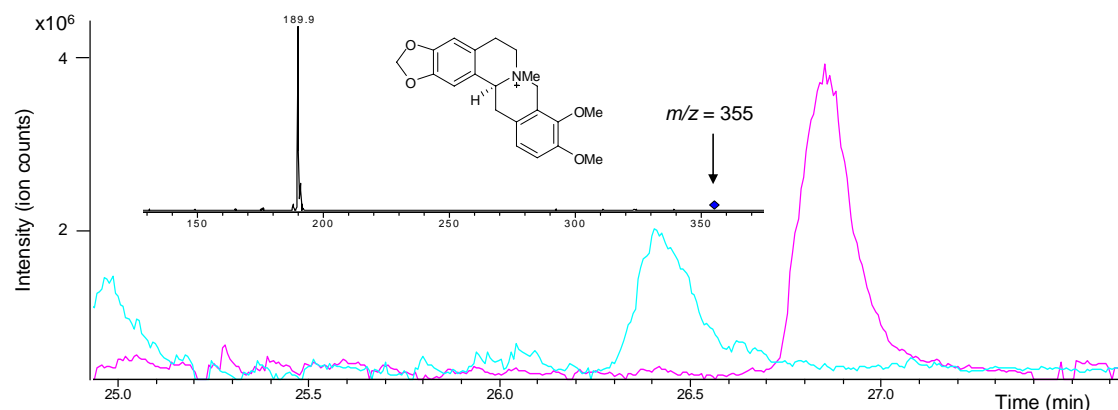


Fig. 4.14. Activity of TNMT on (*S*)-tetrahydroberberine. The product is identified as the $m/z = 355$ ion shown in cyan and elutes as 26.4 min. The major fragment $m/z = 189.9$ is 15 units higher than that from (*S*)-tetrahydroberberine (Fig. 4.10) as expected from the addition of the N-methyl group. The substrate (*S*)-tetrahydroberberine produced *in vivo* in yeast is shown in magenta.

4.2.6. Pathway for laudanine production

An additional branch extending from reticuline which is only known to include one additional step is the AdoMet-dependent methylation in the 7-*OH* position. The *P. somniferum* (*R, S*)-reticuline 7-*O*-methyltransferase converts reticuline to laudanine (Fig. 4.15a). The recombinant 7OMT is slightly more promiscuous than similar plant methyltransferases in that it accepts phenolic compounds; however, it does not accept *N*-demethylated substrates.

This reaction was anticipated to be straightforward in our system; however, yeast strains engineered to express 7OMT from various constructs did not show production of laudanine detectable by LC-MS/MS analysis. *In vitro* reactions set up as described previously⁶⁷ using yeast lysates containing 7OMT also did not show activity of this protein on reticuline, laudanosoline, or guaiacol. Although expression of the full-length protein was confirmed (Fig. 4.15b), no activity was observed under any conditions tested when this cDNA was expressed in yeast.

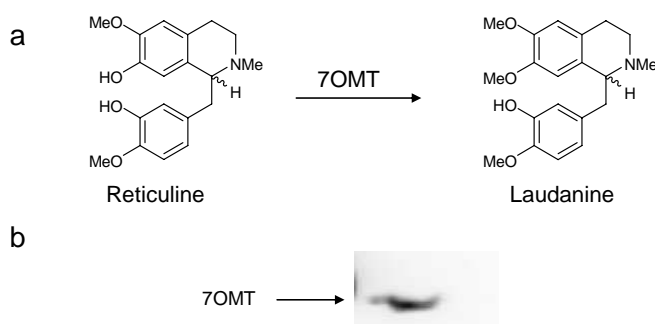


Fig. 4.15. (*R, S*)-Reticuline 7OMT reaction and expression in yeast. **(a)** The reaction performed by 7OMT to convert reticuline to laudanine. **(b)** Expression of the full-length 7OMT in reticuline-producing strain backgrounds was confirmed by Western blotting using a construct tagged with the V5 epitope.

4.2.6. Synthesis of the morphinan intermediate salutaridine

The morphinan alkaloids comprise another major family of BIA metabolites derived from the intermediate reticuline. This family of alkaloids, which includes morphine, codeine, and thebaine, has received the widest pharmacological use to-date and generated interest mainly for their analgesic properties. However, several of the enzymes that perform the early conversion steps in the morphinan branch have not been cloned and characterized, precluding engineering efforts relying on the native enzymes. To further demonstrate the diversity of small molecule products that can be synthesized and the power of reconstructing metabolic pathways in engineered hosts, we utilized an enzyme unrelated to the plant BIA pathway to synthesize an early metabolite in the morphinan branch.

Metabolites in the morphinan branch are synthesized from (*S*)-reticuline via (*R*)-reticuline following a two step-isomerization process (Fig. 4.16a). In the first step, (*S*)-reticuline is transformed to 1,2-dehydroreticuline by 1,2-dehydroreticuline synthase (DRS)⁷². The second step is a reduction of 1,2-dehydroreticuline in the presence of NADPH to (*R*)-reticuline catalyzed by 1,2-dehydroreticuline reductase (DRR)⁷³. Both enzymes have been partially purified and characterized but no sequence information is available to facilitate expression in a recombinant host⁶. With the lack of available cDNAs for enzymes performing the early isomerization steps, engineering a heterologous pathway to produce morphinan alkaloids is not possible if only (*S*)-reticuline is produced. However, using (*R, S*)-norlaudanosoline as the substrate for our engineered BIA pathway resulted in the synthesis of both forms of reticuline, allowing access to metabolites along the branch extending towards morphine production.

The first morphinan alkaloid synthesized from (*R*)-reticuline is salutaridine via a complex carbon-carbon phenol coupling reaction catalyzed by salutaridine synthase. This enzyme was recently cloned from *P. somniferum* but no characterization studies have been published to date^{6, 74}. However, a recent study demonstrating that humans are capable of synthesizing small amounts of morphine suggests the presence of analogous enzymes in other organisms. The human cytochrome P450 CYP2D6 has been implicated in this pathway, specifically catalyzing the hydroxylation of tyramine to dopamine and the demethylation of codeine to morphine⁷⁵. Furthermore, it was implied that an unidentified P450 enzyme, possibly CYP2D6, may accept reticuline as a substrate although experimental evidence was not shown. We examined the ability of CYP2D6 to convert (*R*)-reticuline to salutaridine in our engineered yeast strains (Fig. 4.16b). We constructed plasmids expressing the *CYP2D6* cDNA and various reductase partners for co-expression in our reticuline-producing yeast strain backgrounds (CSY463, CSY465-6; Table 4.1).

LC-MS/MS analysis demonstrated that CYP2D6 catalyzed the conversion of (*R*)-reticuline to salutaridine in strains producing (*R, S*)-reticuline, highlighting a previously uncharacterized activity for this enzyme (Fig. 4.16b). Surprisingly, this reaction proceeded with only endogenous levels of the yeast P450 reductase (yCPR) and observed levels of salutaridine in a CSY288 background strain were consistent with 6-8% conversion of (*R, S*)-reticuline. Codon-optimization of the CYP2D6 sequence (yCYP2D6) to improve translational efficiency in yeast did not show a significant improvement in salutaridine yield but was retained for future work to help lighten metabolic burden of this extensive pathway (Fig. 4.16c). Based on our experience with the CYP719A cofactor

expression system, a chromosomal integration of the *hCPR1* reductase gene was made in the reticuline-producing background strain. This resulted in a ~30% increase in salutaridine production which was further increased by expressing *yCYP2D6* from the TEF6 promoter with 1.2 times the transcriptional activity of the native TEF1 promoter. Additional strains constructed with the soluble *yCPRΔ33* and a fusion of the *yCYP2D6-yCPRΔ33* did yield additional improvements. The maximum yield of salutaridine based on ~15% conversion of reticuline is ~25 mg l⁻¹ from 5 mM norlaudanosoline. However, the activity of CYP2D6 on (*R*)-reticuline remained relatively low as cofactor and expression optimization strategies yielded only modest improvements. As human P450 enzymes are notoriously promiscuous, the affinity is likely low for (*R*)-reticuline and may require additional protein engineering or evolution to significantly improve specificity and activity for this substrate. In addition, as enzymes that exhibit this activity are cloned and characterized from plant hosts, they can be tested in our system for increased production of salutaridine⁷⁴.

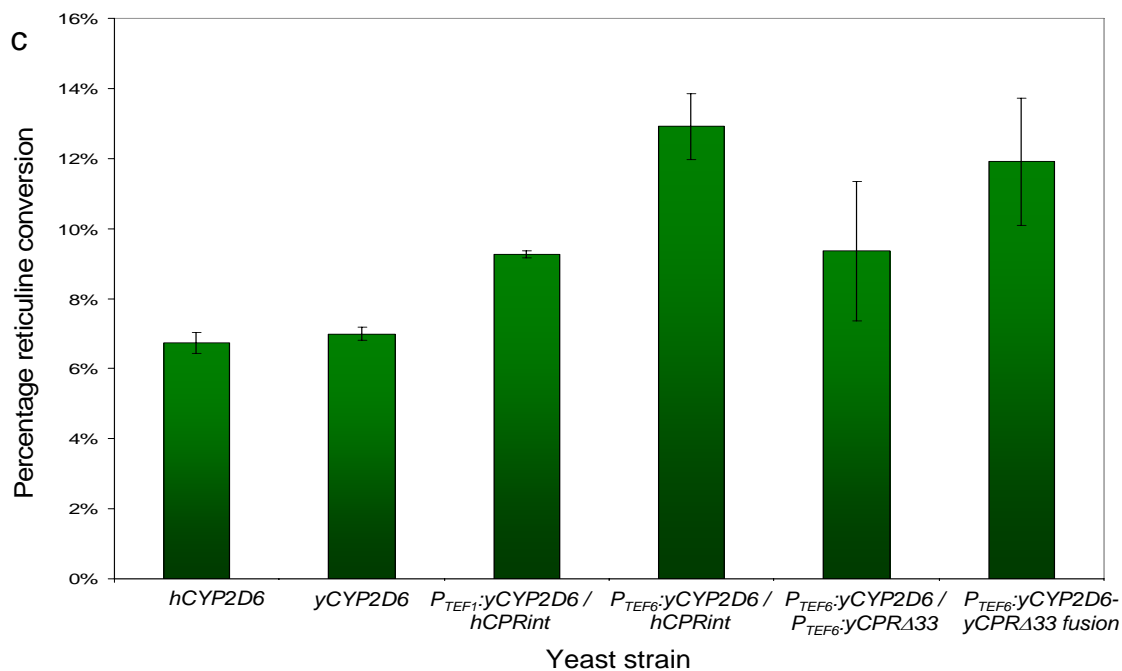
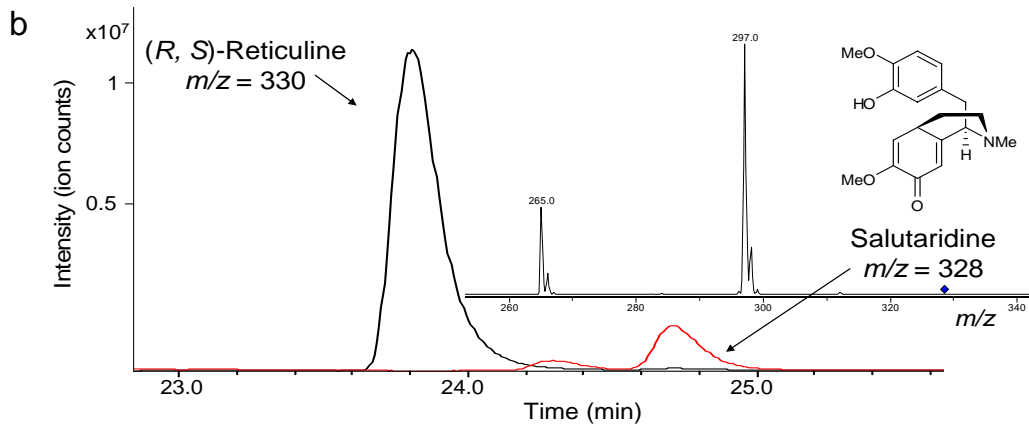
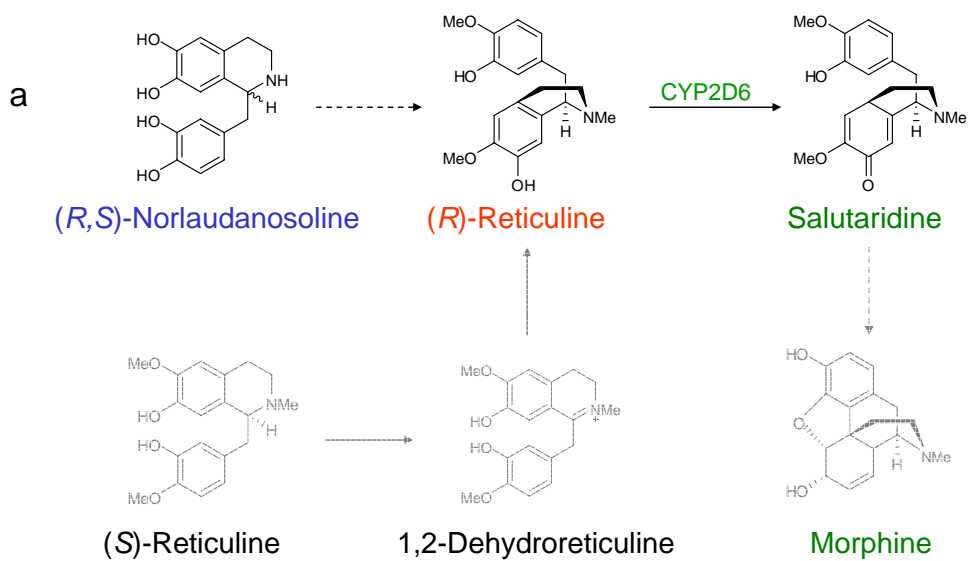


Fig. 4.16. Microbial production of morphinan alkaloids. **(a)** Native and engineered pathways for the synthesis of morphinan metabolites. Color schemes and notation follow that defined in Fig. 4.1. In the engineered pathway, (*R*)-reticuline is produced from (*R*)-norlaudanosoline. A heterologous human cytochrome P450 (*CYP2D6*) enzyme can convert (*R*)-reticuline to the first morphinan alkaloid salutaridine. In the native plant pathway, only (*S*)-reticuline is produced and two additional enzymes are required to produce (*R*)-reticuline, which is used in the synthesis of the morphinan alkaloids. **(b)** LC-MS/MS analysis of the growth media of engineered yeast strains supplemented with 4 mM norlaudanosoline and grown for 48 h confirms salutaridine production. Extracted ion chromatograms are shown for reticuline (black) and salutaridine (red) produced by CSY489 and are representative of analogous strains. The salutaridine 328 ion elutes at the same time as (*S*)-scoulerine, but exhibits a distinctly different fragmentation pattern. The major ions ($m/z = 297$ and 265) are consistent with the expected fragments reported in the literature for salutaridine⁷⁶. Strains lacking the *CYP2D6* coding sequence did not produce the metabolite peak identified as salutaridine. **(c)** Multiple salutaridine-producing strains were tested for conversion of reticuline to salutaridine. The *x*-axis shows the *CYP2D6* and *CPR* expression constructs present in the CSY288 background strain. The ‘optimal’ strain (which includes consistency) contains a chromosomal integration of *hCPR1* and increased plasmid-based expression of γ *CYP2D6*.

4.3. Discussion

The implementation of synthetic BIA pathways in a microbial host represents a significant challenge and a rich area for future research, in part due to the complex enzyme activities and regulatory strategies present in the plant hosts that may not translate directly to the engineered host by simply expressing the cloned enzyme activities. For example, a major factor that may generally limit enzymatic activity and conversion is the lack of subcellular compartmentalization in yeast. In particular, BBE and other enzymes are believed to be associated with endomembranes, forming ‘vesicles’ or ‘metabolons’ that facilitate channeling of intermediates and sequestration of toxic metabolites from the cytosol⁷⁷. Future engineering efforts may enable the assembly of synthetic enzyme complexes in heterologous hosts. A second factor that may limit conversion is the prevalence of cytochrome P450s in the native pathway, which typically exhibit low to no activity in microorganisms. Both *CYP719A1* and *CYP2D6* exhibited

significantly improved activities when coupled to the appropriate reductase partner stably integrated into the host genome as opposed to plasmid-based expression. However, both P450 enzymes did not fully consume their substrates, highlighting the potential for yield improvements at these steps through protein engineering strategies. A third factor that may limit conversion is the lack of an active transport system to facilitate passage of BIA metabolites across microbial cell membranes and allow for higher intracellular substrate concentrations. Such limitations highlight the importance for reconstruction of these pathways in a single microbial host and may represent a target for future engineering efforts to improve uptake of synthetic substrates.

As a heterologous production host for diverse BIA molecules, our engineered strains will be useful tools in furthering the characterization of a ubiquitous plant secondary metabolic pathway. First, our strains can be used as tools to characterize enzymes and probe regulatory strategies for the BIA pathway in a synthetic host. For example, we utilized our strains to probe the relative activities of enzyme variants in the engineered pathway. We further described the application of a general tool for titrating individual pathway enzymes to determine optimal expression levels. Such strategies indicated that the 6OMT and CNMT variants from *P. somniferum* exhibited superior properties in the engineered pathways relative to the *T. flavum* variants. Second, our strains can be used as functional genomics tools to further the elucidation of the BIA pathway and characterize new enzyme activities from native plant hosts or non-native sources as demonstrated here. The engineered strains can be used to screen cDNA libraries from BIA-producing plants in high-throughput assays for activities that modify

BIA metabolites. Such a tool is particularly powerful in light of the scarce availability of many BIA intermediates and challenges in plant metabolic engineering.

We have constructed unique production hosts for a diverse set of BIAs offering access to a large family of pharmacologically-relevant molecules previously unattainable from other natural sources and synthetic chemistry approaches. Our production hosts offer advantages in directing the production of specific BIA molecules, ease of purification from a GRAS organism, well-established fermentation schemes, and rapid biomass accumulation. The microbial BIA production levels reported here reached ~ 150 mg l⁻¹, similar to previously reported yields from initial engineering efforts on microbial strains to produce other natural plant products⁷⁸. The application of industrial optimization strategies is expected to significantly increase production levels. More importantly, the engineered yeast strains offer the potential to produce an even broader spectrum of BIA metabolites through extensions of this synthetic pathway. For example, as new enzyme activities are cloned from the native plant hosts, the cDNAs can be expressed in our engineered strains to produce berberine and other BIA metabolites in the sanguinarine, morphinan, and bis-benzylisoquinoline branches. As demonstrated here with a human P450 enzyme, there is also the exciting potential to express enzymes unrelated to the native BIA pathway but that accept BIA metabolites as substrates in our synthetic hosts to access a wider pool of intermediates and derivatives. Furthermore, strategies that involve recombining native and novel enzyme activities and feeding alternative substrates can be used to produce non-natural BIA molecules, expanding molecular diversity. Finally, synthetic methods can be used in conjunction with *in vivo* biosynthesis to attach various functional groups to the molecular backbones, thereby

creating a rich population of alkaloids and potentially tapping into new and enhanced pharmacological activities.

4.4. Materials and Methods

4.4.1. Plasmid and yeast strain construction

We obtained restriction enzymes, T4 DNA ligase, and other cloning enzymes from New England Biolabs. We performed polymerase chain reaction (PCR) amplifications using Expand High Fidelity PCR System (Roche). Oligonucleotide synthesis was performed by Integrated DNA Technologies. A list of strains and primer sequences for chromosomal integrations is provided (Tables 4.1 and 4.2).

Table 4.1. Engineered yeast strains.

<u>Strain</u>	<u>Integrated constructs</u>	<u>Plasmid-based constructs</u>
CSY288	<i>his3::P_{TEF1}-Ps6OMT, leu2::P_{TEF1}-PsCNMT, ura3::P_{TEF1}-Ps4'OMT</i>	
CSY307		<i>P_{TEF1}-Ps6OMT, P_{TEF1}-PsCNMT, P_{TEF1}-Ps4'OMT</i>
CSY308		<i>P_{TEF1}-Ps6OMT, P_{TEF1}-TfCNMT, P_{TEF1}-Ps4'OMT</i>
CSY309		<i>P_{TEF1}-Tf6OMT, P_{TEF1}-PsCNMT, P_{TEF1}-Ps4'OMT</i>
CSY310		<i>P_{TEF1}-Tf6OMT, P_{TEF1}-TfCNMT, P_{TEF1}-Ps4'OMT</i>
CSY311		<i>P_{TEF1}-Ps6OMT, P_{TEF1}-PsCNMT, P_{TEF1}-Tf4'OMT</i>
CSY312		<i>P_{TEF1}-Ps6OMT, P_{TEF1}-TfCNMT, P_{TEF1}-Tf4'OMT</i>
CSY313		<i>P_{TEF1}-Tf6OMT, P_{TEF1}-PsCNMT, P_{TEF1}-Tf4'OMT</i>
CSY314		<i>P_{TEF1}-Tf6OMT, P_{TEF1}-TfCNMT, P_{TEF1}-Tf4'OMT</i>
CSY325	<i>his3::P_{GAL1-10}-Ps6OMT-loxP-Kan^R, leu2::P_{TEF1}-PsCNMT, ura3::P_{TEF1}-Ps4'OMT, gal2::HIS3</i>	
CSY326	<i>his3::P_{TEF1}-Ps6OMT, leu2::P_{TEF1}-PsCNMT, ura3::P_{GAL1-10}-Ps4'OMT-loxP-LEU2, gal2::HIS3</i>	
CSY327	<i>his3::P_{TEF1}-Ps6OMT, leu2::P_{GAL1-10}-PsCNMT-loxP-URA3, ura3::P_{TEF1}-Ps4'OMT, gal2::HIS3</i>	
CSY328	<i>his3::P_{TEF1}-Ps6OMT, leu2::P_{TEF1}-PsCNMT, ura3::P_{GAL1-10}-Tf4'OMT-loxP-LEU2, gal2::HIS3</i>	
CSY329	<i>his3::P_{GAL1-10}-Tf6OMT-loxP-LEU2, leu2::P_{TEF1}-PsCNMT, ura3::P_{TEF1}-Tf4'OMT, gal2::HIS3</i>	
CSY334	<i>his3::P_{TEF1}-Ps6OMT, leu2::P_{TEF1}-PsCNMT, ura3::P_{TEF1}-Tf4'OMT</i>	
CSY336	<i>his3::P_{TEF1}-Ps6OMT, leu2::P_{TEF1}-PsCNMT, ura3::P_{TEF1}-Ps4'OMT</i>	<i>P_{TEF1}-PsBBE</i>
CSY337	<i>his3::P_{TEF1}-Ps6OMT, leu2::P_{TEF1}-PsCNMT, ura3::P_{TEF1}-Ps4'OMT</i>	<i>P_{TEF1}-PsBBE, P_{TEF1}-TfS9OMT</i>
CSY338	<i>his3::P_{TEF1}-Ps6OMT, leu2::P_{TEF1}-PsCNMT, ura3::P_{TEF1}-Tf4'OMT</i>	<i>P_{TEF1}-PsBBE</i>
CSY339	<i>his3::P_{TEF1}-Ps6OMT, leu2::P_{TEF1}-PsCNMT, ura3::P_{TEF1}-Tf4'OMT</i>	<i>P_{TEF1}-PsBBE, P_{TEF1}-TfS9OMT</i>
CSY399	<i>his3::P_{TEF1}-Ps6OMT, leu2::P_{TEF1}-PsCNMT, ura3::P_{TEF1}-Ps4'OMT</i>	<i>P_{TEF1}-PsBBE, P_{TEF1}-TfS9OMT, P_{TEF1}-TfCYP719A, P_{TEF1}-AtATR1</i>
CSY400	<i>his3::P_{TEF1}-Ps6OMT, leu2::P_{TEF1}-PsCNMT, ura3::P_{TEF1}-Tf4'OMT</i>	<i>P_{TEF1}-PsBBE, P_{TEF1}-TfS9OMT, P_{TEF1}-TfCYP719A, P_{TEF1}-AtATR1</i>
CSY410	<i>his3::P_{TEF1}-Ps6OMT, leu2::P_{TEF1}-PsCNMT, ura3::P_{TEF1}-Ps4'OMT, trp1::P_{TEF1}-AtATR1-loxP-Kan^R</i>	<i>P_{TEF1}-PsBBE, P_{TEF1}-TfS9OMT, P_{TEF1}-TfCYP719A</i>
CSY424	<i>his3::P_{TEF1}-Ps6OMT, leu2::P_{TEF1}-PsCNMT, ura3::P_{TEF1}-Tf4'OMT</i>	<i>P_{TEF1}-yCYP2D6</i>
CSY425	<i>his3::P_{TEF1}-Ps6OMT, leu2::P_{TEF1}-PsCNMT, ura3::P_{TEF1}-Ps4'OMT, trp1::P_{TEF1}-AtATR1-loxP-Kan^R</i>	<i>P_{TEF1}-yCYP2D6</i>
CSY428	<i>ura3::P_{TEF1}-yEGFP3-loxP-LEU2</i>	
CSY429	<i>ura3::P_{GAL1-10}-yEGFP3-loxP-LEU2, gal2::Kan^R</i>	
CSY448	<i>his3::P_{TEF7mut}-Ps6OMT, leu2::P_{TEF7mut}-PsCNMT, ura3::P_{TEF7mut}-Ps4'OMT</i>	
CSY449	<i>his3::P_{TEF7mut}-Ps6OMT, leu2::P_{TEF7mut}-PsCNMT, ura3::P_{TEF7mut}-Tf4'OMT</i>	
CSY450		<i>P_{TEF1}-Ps6OMT</i>
CSY451		<i>P_{TEF1}-Tf6OMT</i>
CSY452		<i>P_{TEF1}-PsCNMT</i>
CSY453		<i>P_{TEF1}-TfCNMT</i>
CSY454		<i>P_{TEF1}-Ps4'OMT</i>
CSY455		<i>P_{TEF1}-Tf4'OMT</i>
CSY456	<i>his3::P_{TEF1}-Tf6OMT, leu2::P_{TEF1}-PsCNMT, ura3::P_{TEF1}-Tf4'OMT</i>	
CSY458	<i>his3::P_{TEF7mut}-Tf6OMT, leu2::P_{TEF7mut}-PsCNMT, ura3::P_{TEF7mut}-Tf4'OMT</i>	
CSY463	<i>his3::P_{TEF1}-Ps6OMT, leu2::P_{TEF1}-PsCNMT, ura3::P_{TEF1}-Tf4'OMT</i>	<i>P_{TEF1}-hCYP2D6</i>
CSY464	<i>his3::P_{TEF1}-Ps6OMT, leu2::P_{TEF1}-PsCNMT, ura3::P_{TEF1}-Tf4'OMT</i>	<i>P_{TEF1}-yCYP2D6:yCPR1 (fusion protein)</i>
CSY465	<i>his3::P_{TEF1}-Ps6OMT, leu2::P_{TEF1}-PsCNMT, ura3::P_{TEF1}-Ps4'OMT</i>	<i>P_{TEF1}-hCYP2D6, P_{TEF1}-yCPR1</i>
CSY466	<i>his3::P_{TEF1}-Ps6OMT, leu2::P_{TEF1}-PsCNMT, ura3::P_{TEF1}-Ps4'OMT</i>	<i>P_{TEF1}-hCYP2D6, P_{TEF1}-AtATR1</i>
CSY489	<i>his3::P_{TEF1}-Ps6OMT, leu2::P_{TEF1}-PsCNMT, ura3::P_{TEF1}-Ps4'OMT, trp1::P_{TEF1}-hCPR-loxP-LEU2</i>	<i>P_{TEF1}-hCYP2D6</i>
CSY490	<i>his3::P_{TEF1}-Ps6OMT, leu2::P_{TEF1}-PsCNMT, ura3::P_{TEF1}-Ps4'OMT</i>	<i>P_{TEF1}-hCYP2D6:hCPR1 (fusion protein)</i>

We used standard molecular biology techniques to construct the BIA expression vectors⁵⁹. BIA expression constructs contained the 2 μ high-copy yeast origin of replication along with appropriate yeast selection markers and ampicillin resistance. Recombinant enzymes were expressed from the yeast TEF1 promoter and flanked by a CYC1 terminator sequence. We constructed shuttle vectors for subcloning of 1 or 2 cDNA sequences in this fashion. Coding sequences for the enzymes of interest, with the exception of *hCYP2D6*, were generously donated as cDNAs from Peter Facchini

(University of Calgary) in plasmids typically suited for expression in *E. coli*. The *hCYP2D6* cDNA was provided by F. Peter Guengerich (Vanderbilt University) as pCW/DB6⁶⁰ and the yeast codon-optimized version of this gene was synthesized by DNA 2.0. We PCR-amplified the endogenous yeast P450 reductase gene (*CPR1*) from W303 genomic DNA, the *A. thaliana ATR1* gene from WAT11 genomic DNA⁷⁹, and the *Homo sapiens CPR1* gene from pH2E1red⁶¹.

We transformed ligation reactions into an electrocompetent *E. coli* strain, DH10B (Invitrogen; F-*mcrA* Δ (*mrr-hsdRMS-mcrBC*) ϕ 80*lacZ* Δ M15 Δ *lacX74 deoR recA1 endA1 araD139 Δ (*ara, leu*)7697 *galU galK λ -rpsL nupG*), using a Gene Pulser Xcell System (BioRAD) according to the manufacturer's instructions. We conducted plasmid isolation using the Wizard Plus SV Minipreps DNA purification system (Promega) according to the manufacturer's instructions. Subcloning was confirmed by restriction analysis and sequence verification (Laragen, Inc.). We transformed plasmids into the appropriate *S. cerevisiae* strains using a standard lithium acetate protocol⁶². All yeast strains used in this work were based on the haploid yeast strain W303 α (*MAT α his3-11,15 trp1-1 leu2-3 ura3-1 ade2-1*)⁶³. *E. coli* cells were grown on Luria-Bertani media (BD Diagnostics) with 100 μ g/ml ampicillin (EMD Chemicals) for plasmid maintenance, and *S. cerevisiae* cells were grown in synthetic complete media (BD Diagnostics) supplemented with the appropriate dropout solution for plasmid maintenance (Calbiochem).*

We performed chromosomal integrations of DNA fragments through homologous recombination using a standard lithium acetate transformation protocol to construct strains that stably express combinations of the BIA enzymes. We built gene insertion

cassettes harboring the appropriate BIA enzyme expression construct and associated selection marker flanked by *loxP* sites to allow removal of the selection marker following integration with a Cre-*loxP* system⁸⁰. The plasmids pUG6, pUG27, pUG72, and pUG73⁸¹ (EUROSCARF) contain geneticin resistance, *S. pombe his5⁺*, *Kluyveromyces lactis URA3*, and *K. lactis LEU2* genes, respectively, flanked by *loxP* sites and were used in the construction of the integration cassettes. We amplified and assembled the TEF1 promoter and CYC1 terminator using PCR-based methods and the primers TEF.fwd, TEF.rev, CYC1.fwd, and CYC1.rev (Table 4.2). The assembled DNA insert contained a multi-cloning site and was subcloned upstream of the selection marker in each construct. We cloned cDNAs into the multi-cloning site and amplified the entire integration cassette in two PCR steps using “A” and “B” primer sets to add ~80 nt of homology (Table 4.2). We gel purified integration cassettes using the Zymoclean Gel DNA Recovery Kit (Zymo Research) according to the manufacturer’s instructions prior to transformation into the appropriate yeast strain. Integration of the cassettes into the correct locus was confirmed by PCR analysis of the targeted region of the chromosome. To remove all selection markers from the final strains, we transformed cells with the plasmid pSH63 which expresses a GAL-inducible Cre recombinase⁸¹. Cells harboring the plasmid were induced with galactose for 24 h and then transferred to YPD media to remove the selection pressure for plasmid maintenance. We isolated and restreaked single colonies on appropriate media to verify the loss of selection markers.

We built template plasmids for chromosomal integrations for the enzyme titration studies by cloning the GAL1-10 promoter (amplified from pRS314-GAL³⁸ using primers GAL.fwd and GAL.rev) in place of the TEF1 promoter in pUG-based plasmids.

Construction of strains using the GAL1-10 promoter to control expression of single enzymes was analogous to that described for the TEF1 promoter strains with a final step to replace the *GAL2* locus with the *his5*⁺ selection marker using a cassette amplified from pUG27 with primers GAL2ko.fwd and GAL2ko.rev. We confirmed integration into the targeted site with primers GAL2sc.fwd and GAL2sc.rev (Table 4.2).

Table 4.2. Primer sequences used for qRT-PCR and to make stable integrations of enzyme constructs and *GAL2* knockouts. Restriction sites are underlined.

Primer name	Sequence
TEF.fwd	ATAAAAGC <u>TTACATATGCATAGCTT</u> CAAAATGTTTCTACTCC
TEF.rev	TGCTAGC <u>GTTTAAACGAATTCTGGATCCATCCTAGG</u> AAAACTTAGATTAGATTGCTATGC
CYC1.fwd	ATGGATCCAGAA <u>TTTCGTTTAAACG</u> CTAGCACCCGGGGAGGGCCGCATCATGTAATTAGTT
CYC1.rev	ATAACTGCAGAG <u>TCGACGGCCG</u> CAAATTAAGCCTTCGA
HISint.fwdA	TATACTAAAAATGAGCAGGTGTCGGGGCTGGCTTAACTATGCGGCATCA
HISint.revA	TATATATATCGTATGCTGCAGCTCTGGCTTATCGAAATTAATACGACTCACTA
HISint.fwdB	ATTGGCATTATCACATAATGAATTATACATTATATAAGTAATGTGATTTCTTGAAGAATATACTAAAAATGAGCAGG
HISint.revB	AGTATCATACTGTTTCGTATACATACTTACTGACATTCATAGGTATACATATATACACATGTATATATATCGTATGCTGCAGCT
LEUint.fwdA	AGCAATATATATATATATATTGTCGGGGCTGGCTTAACTATGCGGCATCA
LEUint.revA	AGTTTATGTACAAATATCATAA <u>CTGGCTTATCGAAATTAATACGACTCACTA</u>
LEUint.fwdB	TTTTCCAATAGGTGTTAGCAATCGTCTTACTTTCTAACTTTTCTTACCTTTTACATTTTCAGCAATATATATATATATAT
LEUint.revB	TACCCTATGAACATATTCCATTTTGTAAATTCGTGTCGTTTCTATTATGAATTTTCATTATAAAGTTTATGTACAAATATCATAA
URAint.fwdA	ACTGCACAGAACAACCTTGTGGGGCTGGCTTAACTATGCGGCATCA
URAint.revA	AGTTTAGTATACATGCATTTACTGGCTTATCGAAATTAATACGACTCACTA
URAint.fwdB	GGTATATATACGCATATGTGGTGTGAAGAACATGAAATTGCCAGTATTCTTAACCAACTGCACAGAACAACCT
URAint.revB	AATCATTACGACCGAGATTCCCGGTAATAACTGATATAAATAAATGAAGCTCTAATTTGTGAGTTTAGTATACATGCATTTA
GAL.fwd	ATAAAGC <u>TTACATATG</u> TCTAGAAAATTCCTTGAATTTTCAAAAAT
GAL.rev	ATAC <u>CTAGG</u> TTTTTTCTCCTTGACGTTAAAGTATAGAG
GAL2ko.fwd	CATTAATTTTGCTTCCAAGACGACAGTAATATGTCTCCTACAATACCAGTGTGGGGCTGGCTTAACTATGCGGCATCA
GAL2ko.rev	TATATGTACACAAATAATAGGTTTAGGTAAGGAATTTATATAATCGTAAGCTGGCTTATCGAAATTAATACGACTCACTA
GAL2sc.fwd	TGTGCATGTTATCTATATCCTTCTTTATATAGATGCTGTT
GAL2sc.rev	ATTAATTGTATGTTAGCTCAGGAATTCAACTGGAAGAAAG

4.4.2. Growth conditions

For BIA metabolite production assays with the exception of enzyme titration studies, engineered yeast strains were grown in test tube cultures in volumes ranging from 2-10 mL at 30°C and 200 rpm in the appropriate drop out media with 2% dextrose

(w/v) as a sugar source. We diluted overnight cultures 1:20 in fresh media supplemented with the appropriate pathway substrate as reported, typically norlaudanoline (CHEMOS GmbH, ACROS Organics; ~\$160 g⁻¹) or laudanoline (ACROS Organics; ~\$220 g⁻¹) at concentrations between 0.1-5 mM diluted from a 10 or 20 mM stock solution in water. With the exception of time-course experiments, we assayed cultures at 24 or 48 h following substrate addition to observe maximum accumulation as cells reached the stationary growth phase.

For the enzyme titration assays, GAL-inducible strains were grown overnight in synthetic complete media containing all amino acids with 2% raffinose (w/v), 1% sucrose (w/v) as a sugar source. Galactose was added to the media at the appropriate concentration from a 10X stock at the time of back dilution and the norlaudanoline substrate was added to a final concentration of 1 mM following an induction period of 4 h. We sampled aliquots of the growth media for LC-MS/MS analysis 24 h after substrate addition. Data is reported as reticuline production measured by LC-MS peak area.

4.4.3. Analysis of metabolite production

We evaluated BIA metabolite levels by LC-MS/MS analysis of cell extracts and growth media. At appropriate time points, aliquots of yeast cultures were centrifuged to recover cells as pellets and allow collection of the growth media. We analyzed the growth media or an appropriate dilution directly by LC-MS/MS. Samples were run on an Agilent ZORBAX SB-Aq 3 x 250 mm, 5 μm column with 0.1% acetic acid as solvent A and methanol as solvent B. We used a gradient elution to separate the metabolites of interest as follows: 0-10 min at 100% A, 10-30 min 0-90% B, 30-35 min 90-0% B, followed by a

5 min equilibration at 100% A between samples. Following LC separation, metabolites were injected into an Agilent 6320 ion trap MSD for detection and identification. We used selective reaction monitoring to isolate ions of interest for MS/MS to verify the molecular structure of each metabolite. We verified chromatogram data including fragmentation patterns through at least three independent experiments and from multiple strains where appropriate. Quantification of metabolites was based on the integrated area of the extracted ion chromatogram peaks⁶⁴ calculated using DataAnalysis for 6300 Series Ion Trap LC/MS Version 3.4 (Bruker Daltonik GmbH) and reported as the mean \pm s.d. When appropriate, we normalized the measured levels to a metabolite peak of known concentration in the growth media, typically the substrate (norlaudanosoline) peak. We also generated standard curves for norlaudanosoline and laudanosoline to relate peak area to metabolite concentration in our samples. Although slight differences in ionization efficiencies were observed between these available standards, this method further validated our estimates of metabolite concentrations based on percentage substrate conversion. A summary of the average yields for each of the synthesized BIA compounds is provided (Table 4.3).

Table 4.3. Summary of yields of benzyloquinoline alkaloids. Yields are reported from the supernatant of growth cultures of the appropriate strains fed 5 mM norlaudanosoline.

BIA compound	yield (μM)	yield (mg l⁻¹)
(R, S)-reticuline	500	164.5
(S)-scoulerine	200	65.4
(S)-tetrahydrocolumbamine	200	68.2
(S)-tetrahydroberberine	100	33.9
salutaridine	75	24.5

4.4.4. Fluorescence quantification

For fluorescence measurements of CSY428 and CSY429, overnight cultures were grown in synthetic complete media with either 2% dextrose or 2% raffinose and 1% sucrose (noninducing-nonrepressing), respectively. Cells were backdiluted into fresh media containing either dextrose (CSY428) or noninducing-nonrepressing media supplemented with the appropriate galactose concentration from a 10X stock (CSY429). We measured fluorescence (excitation 485 nm, emission 515 nm) and OD₆₀₀ values on a fluorescence plate reader (TECAN, Safire). Fluorescence values were normalized using the OD₆₀₀ reading and values from a no stain control (wild-type cells) were subtracted. We used the resulting trend between relative fluorescence and galactose concentration as a guideline to estimate relative protein expression levels in our titratable strains.

4.4.5. Analysis of protein levels through Western blotting

We constructed plasmids for Western blotting experiments by cloning the C-terminal epitope tag(s) from pYES-NT/A (Invitrogen) into a standard BIA expression vector followed by subcloning of the enzyme of interest. We transformed individual plasmids into wild-type yeast cells using a standard lithium acetate protocol. Overnight cultures were grown and backdiluted 1:100 into 100 ml cultures. Cells were grown to OD₆₀₀ ~1.2 and pelleted by centrifugation. The media was removed and cells were washed in 1 ml PBS, pelleted, and resuspended in 0.5 ml Y-PER plus HALT protease inhibitor (Pierce). Cells were vortexed for ~20 min and the lysate separated by centrifugation. We estimated total protein using the Coomassie Plus Protein Assay Reagent (Pierce) and loaded ~50 µg of each sample onto a protein gel. We used NuPage 4-12% Bis-Tris gels with MES running buffer and transfer buffer according to the

manufacturer's instructions (Invitrogen). Proteins were blotted onto a nitrocellulose membrane (Whatman) using a semi-dry transfer cell (Bio-Rad) for 20 min at 15 V. We incubated the membrane with the Anti-V5 HRP antibody (Invitrogen) according to the manufacturer's instructions (Invitrogen) with 5% nonfat milk as the blocking agent. Proteins were detected with the West Pico Super Signal Detection kit (Pierce) and imaged on a ChemiDoc XRS system (Bio-Rad). The image shown is representative of at least two independent experiments.

4.4.6. Analysis of transcript levels through qRT-PCR

We extracted total RNA from yeast cells grown in 10 ml cultures to $OD_{600} \sim 0.5$ using standard acid phenol extraction procedures⁸². Briefly, cells were pelleted, frozen in liquid nitrogen, and resuspended in a 50 mM NaOAc (pH 5.2) and 10 mM EDTA buffer. Cells were lysed by adding SDS to a final concentration of 1.6% and equal volume of acid phenol and incubating for 10 min at 65°C with intermittent vortexing. Following cooling on ice, the aqueous phase was extracted and further extraction was carried out with an equal volume of chloroform. RNA samples were ethanol precipitated and resuspended in water, and total RNA was quantified on a NanoDrop according to the manufacturer's instructions. RNA samples were treated with DNase (Invitrogen) according to the manufacturer's instructions.

We performed cDNA synthesis using gene-specific primers (Table 4.4) and Superscript III Reverse Transcriptase (Invitrogen) according to the manufacturer's instructions with 5 μ g total RNA used in each reaction. Relative transcript levels were quantified from the cDNA samples by employing an appropriate primer set and the iQ SYBR Green Supermix (Bio-Rad) according to the manufacturer's instructions on an

iCycler iQ qRT-PCR machine (Bio-Rad). We analyzed the resulting data with the iCycler iQ software according to the manufacturer's instructions. We normalized transcript levels to that of the endogenous *ACT1* gene⁸³ using *ACT1*-specific primers. Data are reported as the mean \pm s.d. from at least two independent experiments.

Table 4.4. Primers used for qRT-PCR.

<u>Primer name</u>	<u>Sequence</u>
RTGFP.fwd	GCCATGCCAGAAGGTTATGT
RTGFP.rev	ACCATTCTTTTGTTCAGCC
RT6OMT.fwd	CTCATTAGCTCCACCAGCTAAGTA
RT6OMT.rev	GGTCAAACCGTCGCCTAAAT
RTCNMT.fwd	CAAAGTGCGGGTTACTACTCTG
RTCNMT.rev	TCCACAGAACTTGTAAGTCCAGT
RT4'OMT.fwd	GGTGCCGATGATACTAGGCA
RT4'OMT.rev	CCATTCCTTCATTAAACAAGTGGC
ACT1.fwd	GGCATCATACCTTCTACAACGAAT
ACT1.rev	GGAATCCAAAACAATACCAGTAGTTCTA

4.4.7. Analysis of stereoisomer forms of BIA metabolites through capillary electrophoresis-based chiral separation

We performed chiral analysis of norlaudanoline, laudanoline, and reticuline using the P/ACE MDQ Capillary Electrophoresis (CE) system (Beckman-Coulter). A bare fused silica capillary (50 μ m i.d.) with 31.0 cm effective length (41 cm total) was used. We tested buffer solutions from the chiral test kit (Beckman) with the substrates norlaudanoline and laudanoline and optimized conditions using the HS- β -CD separation buffer at 5% (w/v) according to the manufacturer's instructions. Injection was for 5 psi for 10 sec and voltage separation was performed at 15 kV. A diode array detector (PDA) module was used with the spectra presented taken at 280 nm.

For analysis of reticuline and other BIA metabolites, we developed HPLC methods to use water as the aqueous buffer rather than 0.1% acetic acid to avoid unnecessary noise in the CE spectra. Samples were run on a ZORBAX SB-Aq 3 x 250 mm, 5 μ m column with a gradient elution from 10% B to 90% B between 0 and 30 min where solvent B is methanol and solvent A is water. Reticuline elutes at 13 min using this method as confirmed by MS data. We collected fractions from 13.0-13.2 min and verified purity by re-running the sample(s) on LC-MS. Multiple fractions were collected and concentrated ~4 to 5-fold prior to CE analysis.

4.4.8. Preparation of cell extracts

We prepared cell extracts by washing the cell pellets three times with PBS, adding 1 ml of cold methanol at -40°C, and vortexing with glass beads to disrupt the cells. Cell debris and glass beads were pelleted by centrifugation. The methanol was transferred to a clean tube and concentrated by evaporation to a final volume approximately equal to that of the original cell mass.